

Low Energy Probes of Physics Beyond the Standard Model

Vincenzo Cirigliano¹ and Michael J. Ramsey-Musolf^{2,3}

¹ Theoretical Division, Los Alamos National Laboratory,
Los Alamos, NM 87545, USA

² Department of Physics, University of Wisconsin-Madison,
1150 University Ave., Madison, WI 53706, USA

³ California Institute of Technology,
Pasadena, CA 91125, USA

December 1, 2021

Abstract

Low-energy tests of fundamental symmetries and studies of neutrino properties provide a powerful window on physics beyond the Standard Model (BSM). In this article, we provide a basic theoretical framework for a subsequent set of articles that review the progress and opportunities in various aspects of the low-energy program. We illustrate the physics reach of different low-energy probes in terms of an effective BSM mass scale and illustrate how this reach matches and, in some cases, even exceeds that accessible at the high energy frontier.

1 Introduction

The search for physics Beyond the Standard Model (BSM) is now at the forefront of particle physics. The Standard Model (SM) itself represents a triumph of 20th century physics, providing a unified description of three of the known forces of nature, a framework for explaining much of what is observed experimentally, and – since its inception – predictions for the existence of new particles such as the top quark that have subsequently been verified. Over the course of its existence, the SM has withstood numerous tests at variety of energy scales, ranging from those associated with atomic processes to energies at the Z -pole and above. Indeed, the level of agreement between SM predictions and electroweak precision observables (EWPOs) – generally at the 10^{-3} level or better – places severe constraints on the BSM mass scale, Λ , though the existence of a few significant disagreements may signal the existence of “new physics” below this scale.

Despite the impressive successes of the SM, there exist strong observational and theoretical reasons to believe that it is part of a larger framework and that the ultimate goal of BSM searches is to develop a “new Standard Model” of nature’s fundamental interactions. From an observational standpoint, the experimentally determined components of the “cosmic energy budget” given some of the strongest indications of BSM physics. Neither the relic abundance of cold dark matter nor the visible matter-antimatter asymmetry can be explained by the SM. The largest fraction of the energy density of the universe – the dark energy – is equally mysterious if not more so¹. The observation of neutrino oscillations and that imply non-vanishing masses for the neutrinos require at least a minimal extension of the original version of the SM. And the discrepancy between the muon anomalous magnetic moment, a_μ , as measured by the E821 Collaboration at Brookhaven National Laboratory and SM expectations – now at the $\gtrsim 3\sigma$ level – could be due to new particles with masses $\lesssim \Lambda$ or below.

Theoretically, it has long been postulated that the known forces of nature (and possibly others) existed as a single unified force at the moment of the Big Bang, thereby incorporating gravity along with the electroweak and strong interactions in a manner outside the SM. In fact, the running couplings of the SM are suggestive of such a situation, leading to a “near miss” for unification at the GUT scale 10^{16} GeV (see below) and hinting at the possibility that the presence of additional particles and/or forces would close the gap. Theorists have also contended for some time with the so-called “hierarchy problem” associated with quadratically divergent quantum corrections to the Higgs boson mass. The most “natural solutions” to this problem point to new physics at the Terascale, though it is not ruled out that Λ is somewhat larger and that some degree of fine-tuning is required. A number of other features of the SM require BSM physics to explain them: the origin of parity-violation in weak interactions; the quantization of electric charge; and values of the input parameters, such as the fermion masses whose spectrum spans eleven orders of magnitude.

The quest for a new Standard Model that addresses these experimental and theoretical puzzles entails effort at three frontiers: the high energy frontier, now comprised by the CERN Large Hadron Collider; the Cosmological frontier, including probes of the cosmic microwave background and large scale structure as well as indirect astrophysical detection of dark matter; and the Intensity or Precision frontier that is the focus of this issue. The Intensity Frontier (IF) is itself an interdisciplinary field of research, involving experimental and theoretical physicists from the atomic, nuclear, and high energy physics communities. In the articles that follow, we emphasize the studies within the nuclear physics community, recognizing that there the lines between these communities are not precisely defined. That being said, we distinguish three classes of studies being pursued by members of the nuclear physics community:

- (a) *Rare and forbidden processes.* Highly suppressed or strictly forbidden in the Standard Model, these observables include permanent electric dipole moments (EDMs) of leptons, nucleons, and

¹However, one may account for the acceleration expansion of spacetime with a cosmological constant.

atoms; the neutrinoless double β -decay of nuclei ($0\nu\beta\beta$); and processes that do not conserve flavor, such as the charged lepton flavor violating (CLFV) decay $\mu \rightarrow e\gamma$. In most cases, the observation of such an observable would provide “smoking gun” evidence for BSM physics, though in the case of EDMs of systems containing quarks the so-called “ θ -term” in the QCD Lagrangian could be responsible.

- (b) *Precision tests.* These studies measure quantities that are allowed within the Standard Model, but do so at a level of precision that could uncover tiny deviations from Standard Model expectations and signal the presence of BSM dynamics. Of particular interest to the nuclear physics community are the weak decays of the muon and hadrons containing light quarks (including heavy nuclei), parity-violating asymmetries in the scattering of polarized electrons from unpolarized targets, and the (anomalous) magnetic moments of the muon and of neutrinos. The interpretation of these measurements in terms of BSM physics depends critically on the reliability of Standard Model predictions as well as the level of experimental precision.
- (c) *Cosmological and astrophysical probes.* The production of neutrinos in astrophysical processes, such as energy production in the sun or supernovae, can provide unique clues about the underlying fundamental physics – as can the analysis of the role played by neutrinos in cosmological processes, such as those responsible for large scale structure. At the other end of the distance scale spectrum, terrestrial experiments exploiting heavy nuclei as detectors give the most sensitive means for detecting the presence of relic dark matter in many scenarios. In both cases, obtaining a sufficiently reliable understanding of the “laboratories” (*e.g.*, the Sun or heavy nuclei) is important for a proper interpretation of these studies in terms of possible BSM dynamics.

In the remainder of this issue, we discuss in detail the theoretical framework for the interpretation of these studies. Our goal is not to review the state of the field experimentally, but rather to provide a theoretical context in which to view the significance of various measurements. This endeavor is particularly timely, given the influx of new results from other frontiers that clearly impacts the significance and interpretation of the IF studies. Indeed, given the dynamic nature of BSM searches, we will not attempt to provide definitive interpretations regarding particular BSM scenarios, but rather to provide a context for the on-going evaluation of the implications of nuclear physics fundamental symmetry tests and neutrino property studies. In this respect, we view this Issue as a providing the background for a working group website that will contain up-do-date information about key experimental results and their interpretation.

The articles that follow are organized according to the outcome of the workshop “Beyond the Standard Model in Nuclear Physics”, held at the University of Wisconsin-Madison in October, 2011 and supported in part by the U.S. Department of Energy Office of Science Nuclear Physics Program and the corresponding office at the National Science Foundation. The workshop was attended by roughly twenty senior and junior theorists from North America, with discussions breaking down into various topical working groups along the lines of the follow articles.

In this introductory article, we first review the Standard Model and its renormalization as applied to the processes of interest here. We subsequently cast the possible effects of BSM physics in the context of effective operators containing the Standard Model fields and possibly a (light) right-handed neutrino. For most purposes, it suffices to concentrate on operators of mass dimension six or lower, whose Wilson coefficients encode the effects of new dynamics at the BSM scale Λ taken to be well above the weak scale $v = 246$ GeV. We conclude with an overview of the discovery potential and diagnosing power of the various probes discussed in depth in the remainder of this volume, emphasizing in each case the theoretical challenges.

Before proceeding, we refer the reader to other recent reviews of these topics, including an earlier article in this journal [1]; a more recent application to supersymmetry [2]; and reviews of EDMs[3],

$0\nu\beta\beta$ [4, 5, 6], ordinary β -decay [7, 8, 9], weak neutral currents[10, 11] as well as hadronic parity-violation [12, 13]. Some of what follows constitutes an update of those earlier works, though the articles in this Issue represent a broader and more thorough treatment.

2 The Standard Model and its Renormalization

2.1 The Lagrangian

As a renormalizable theory, the $SU(3)_C \times SU(2)_L \times U(1)_Y$ Standard Model consists entirely of operators containing mass dimension $d = 4$ that appear in the Lagrangian

$$\mathcal{L}_{\text{SM}} = \mathcal{L}_{\text{gauge}} + \mathcal{L}_{\text{matter}} + \mathcal{L}_{\text{Higgs}} \quad (2.1)$$

where

$$\mathcal{L}_{\text{gauge}} = -\frac{1}{2} \text{Tr} (G_{\mu\nu} G^{\mu\nu}) - \frac{1}{2} \text{Tr} (W_{\mu\nu} W^{\mu\nu}) - \frac{1}{4} B_{\mu\nu} B^{\mu\nu} \quad , \quad (2.2)$$

with $G_{\mu\nu} = T_3^A G_{\mu\nu}^A$, $W_{\mu\nu} = T_2^a W_{\mu\nu}^a$, and $B_{\mu\nu}$ being the $SU(3)_C$, $SU(2)_L$, and $U(1)_Y$ field strength tensors (expressed in terms of the generators T_j^a), and

$$\mathcal{L}_{\text{matter}} = \sum_{f=q,u,d,\ell,e} \bar{f} \not{D} f + \mathcal{L}_Y \quad (2.3)$$

$$\mathcal{L}_{\text{Higgs}} = (D_\mu \varphi)^\dagger D^\mu \varphi - V(\varphi) \quad , \quad (2.4)$$

where the sums run over the left handed quark (lepton) $S(2)_L$ doublets q (ℓ) and right handed quark (lepton) singlets u , d (e)

$$l^i = \begin{pmatrix} \nu_L^i \\ e_L^i \end{pmatrix} \quad e^i = e_R^i \quad q^i = \begin{pmatrix} u_L^i \\ d_L^i \end{pmatrix} \quad u^i = u_R^i \quad d^i = d_R^i \quad , \quad (2.5)$$

and the Higgs doublet φ

$$\varphi = \begin{pmatrix} \varphi^+ \\ \varphi^0 \end{pmatrix} \quad , \quad (2.6)$$

having a potential energy given by $V(\varphi)$. The covariant derivatives are given by

$$D_\mu = \partial_\mu - ig_3 \sum_{A=1}^8 T_3^A G_\mu^A - ig_2 \sum_{a=1}^3 T_2^a W_\mu^a - ig_1 T_1 B_\mu \quad (2.7)$$

with generators $T_1^A = \lambda^A/2$ (acting on quarks only), $T_2^a = \sigma^a/2$, and $T_1 = Y/2$ expressed in terms of the Gell-Mann matrices λ^A , Pauli matrices σ^a , and hypercharge Y (the gauge couplings are alternately denoted $g_s \equiv g_3$, $g \equiv g_2$, and $g' \equiv g_1$). The Yukawa Lagrangian responsible for mass generation through electroweak symmetry-breaking (EWSB) is

$$\mathcal{L}_Y = -Y_u^{jk} \bar{q}_j \epsilon \varphi^* u_k - Y_d^{jk} \bar{q}_j \varphi d_k - Y_\ell^{jk} \bar{\ell}_j \varphi e_k \quad , \quad (2.8)$$

where repeated indices denote a sum over fermion families. Note that we have not included terms responsible for neutrino mass (see below). After EWSB, $\langle 0 | \varphi^T = |0 \rangle = (0, v/\sqrt{2})$ and diagonalization of the Yukawa matrices Y_f^{jk} through the unitarity transformations

$$u_L^j = [S_u]_{jk} U_L^k \quad , \quad d_L^j = [S_d]_{jk} D_L^k \quad , \quad u_R^j = [T_u]_{jk} U_R^k \quad , \quad d_R^j = [T_d]_{jk} D_R^k \quad \text{etc.} \quad (2.9)$$

the flavor diagonal fermion mass matrices are given by

$$m_f = \frac{v}{\sqrt{2}} S_f^\dagger Y_f T_f \quad . \quad (2.10)$$

After the flavor rotations (2.9) the neutral current gauge interactions in Eq. (2.3) remain flavor diagonal, while the charge changing interactions have the form

$$\mathcal{L}_{CC} = -\frac{ig_2}{\sqrt{2}} V_{\text{CKM}}^{jk} \bar{U}_L^j W^+ D_L^k + \text{h.c.} \quad , \quad (2.11)$$

with W_μ^\pm being the charged weak gauge boson fields and

$$V_{\text{CKM}} = S_u^\dagger S_d \quad (2.12)$$

being the Cabibbo-Kobayashi-Maskawa matrix.

The incorporation of non-vanishing neutrino masses as implied by the observation of neutrino oscillations, can be minimally accomplished through the addition to \mathcal{L}_{SM} of either a dimension-four Dirac mass term or a higher dimensional Majorana mass term (or both). The Dirac mass term reads

$$\mathcal{L}_{\text{Dirac}}^\nu = -Y_\nu^{jk} \bar{\ell}_j \epsilon \varphi^* \nu_{Rk} \quad , \quad (2.13)$$

where ν_{Rk} is a right-handed neutrino Dirac spinor field and where the non-vanishing m_ν arises when φ obtains its vev. Like all of the operators appearing in \mathcal{L}_{SM} , the Dirac mass term in Eq. (2.13) has mass dimension four and does not modify the renormalizability of the SM. For $v = 246$ GeV, the Dirac Yukawa couplings Y_ν must have a magnitude $\lesssim 10^{-12}$ to be consistent with the upper bounds on the scale of neutrino masses obtained from cosmology. We will discuss the Majorana mass term in the next section, since it is related to a dimension-five non-renormalizable term in the effective Lagrangian that parameterizes physics beyond the Standard Model.

2.2 Renormalization

A key consideration in the interpretation of low-energy BSM probes is the impact of electroweak radiative corrections on precision observables. When interpreting measurements of electroweak processes performed with 10^{-3} precision or better, reliance on the tree-level SM Lagrangian is not sufficient, as electroweak radiative corrections generically arise at the $\mathcal{O}(\alpha/\pi)$ level. Moreover, in multiple cases the corrections themselves sample momenta at or below the hadronic scale, rendering them susceptible to strong interaction effects and the attendant uncertainties. Consequently, one must devote considerable care in evaluating these corrections and assessing the overall level of theoretical uncertainty. In order to be confident that any deviation from a SM prediction is a *bona fide* indicator of BSM physics, one must have in hand a sufficiently reliable SM computation. Among the better-known examples where strong-interaction effects have challenged the theoretical community are the hadronic vacuum polarization (HVP) and hadronic light-by-light (HLBL) contributions to a_μ ; the $W\gamma$ box graph to neutron and nuclear β -decay; the $Z\gamma$ box graph contribution to the PV asymmetries in elastic ep scattering; and the hadronic contributions to the running of $\sin^2 \theta_W$. In contrast, these issues hold less concern for the interpretation of rare or forbidden processes, as the SM contributions are already sufficiently small to be negligible.

Apart from its importance for obtaining sufficiently reliable SM predictions, the analysis of radiative corrections can also be vital for the assessment of BSM contributions. In the case of SUSY, for example, the imposition of R-parity conservation implies that superpartners contribute to the observables of interest here only via loops. Moreover, if their masses are sufficiently light, then the effective operator

framework described in Section 3 may not be appropriate, as one cannot integrate out these new degrees of freedom at a scale well above the weak scale. In addition, precision measurements at the Z-pole and above constrain various combinations of these loop effects, so one must consistently incorporate these constraints when analyzing the prospective impacts on low-energy processes.

With these considerations in mind, we provide here a brief overview of renormalization in the SM, introducing some formalism that will be of use throughout the remainder of this Issue. In doing so, we largely follow the discussion of Ref. [2]. We generally utilize dimensional regularization with the modified minimal subtraction scheme ($\overline{\text{MS}}$), though the reader should be aware that other schemes (such as on-shell renormalization) are often adopted in the literature². Renormalized quantities are obtained by introducing counterterms that remove the factors of $1/\varepsilon - \gamma + \ln 4\pi$ that arise in divergent one-loop graphs. All $\overline{\text{MS}}$ -renormalized (finite) quantities will be indicated by a hat, as in $\mathcal{O} \rightarrow \hat{\mathcal{O}}$.

Most low energy precision electroweak observables of interest to nuclear physics are mediated at lowest order by the exchange of a virtual gauge boson (GB), so we consider first the renormalization of GB propagators and GB-fermion interactions. We first discuss renormalization relevant to charged current (CC) processes in order to introduce notation and conventions and subsequently discuss the neutral current (NC) sector.

2.3 Charged Current Processes

Radiative corrections to CC amplitudes naturally divide into four topologies: (a) W -boson propagator corrections; (b) corrections to the W -fermion vertices; (c) fermion propagator corrections; and (d) box graphs. There exist extensive studies of these corrections in the SM, dating back to the seminal work of Refs. [14] and the subsequent analysis of Refs. [15, 16, 17, 18]. We refer the reader to these studies and references therein for additional details.

One loop corrections to the W -boson propagator, fermion propagator, and W -fermion vertices are divergent. After renormalization, the W -boson propagator, $iD_{\mu\nu}(k)$ takes the general form in the Feynman gauge

$$iD_{\mu\nu}(k) = -i \left[T_{\mu\nu} \hat{D}_{WW}^T(k^2) + L_{\mu\nu} \hat{D}_{WW}^L(k^2) \right] \quad (2.14)$$

where the transverse and longitudinal projection operators are given by

$$T_{\mu\nu} = -g_{\mu\nu} + k_\mu k_\nu / k^2 \quad (2.15)$$

$$L_{\mu\nu} = k_\mu k_\nu / k^2 \quad (2.16)$$

and $\hat{D}_{WW}^{T,L}(k^2)$ are finite scalar functions. For the low-energy processes of interest here, effects associated with the longitudinal term are suppressed by light fermion masses, so we will not discuss the component further. The renormalized transverse component is given by

$$\left[\hat{D}_{WW}^T(k^2) \right]^{-1} = k^2 - \hat{M}_W^2 + \hat{\Pi}_{WW}^T(k^2) \quad . \quad (2.17)$$

Here \hat{M}_W is the finite part of the bare W -boson mass parameter appearing in the renormalized Lagrangian after electroweak symmetry breaking and $\hat{\Pi}_{WW}^T(k^2)$ gives the finite loop contribution. Both \hat{M}_W and $\hat{\Pi}_{WW}^T(k^2)$ depend on the t'Hooft renormalization scale μ . The physical W -boson mass is μ -independent and is defined by the value of k^2 giving $[\hat{D}_{WW}^T(k^2 = M_W^2)]^{-1} = 0$, *i.e.*, the pole of the propagator.

²Note that in the case of SUSY, one must employ a variation of $\overline{\text{MS}}$ in order to maintain supersymmetry at the loop level. The regulator in this case is dimensional reduction, (DR), wherein one works in $d = 4 - 2\varepsilon$ spacetime dimensions while retaining the Clifford algebra appropriate to fermion field operators in $d = 4$ dimensions. The corresponding renormalization scheme, analogous to $\overline{\text{MS}}$, is known as modified dimensional reduction, or $\overline{\text{DR}}$.

The corresponding expression for the renormalized, inverse fermion propagator is

$$\hat{S}_f^{-1}(k) = \not{k} - \hat{m}_f + \left[\hat{A}_L(k^2)\not{k} + \hat{B}_L(k^2) \right] P_L + \left[\hat{A}_R(k^2)\not{k} + \hat{B}_R(k^2) \right] P_R \quad (2.18)$$

where $P_{L,R}$ are the left- and right-handed projectors and the $\hat{A}_{L,R}$ and $\hat{B}_{L,R}$ contain the finite loop contributions. The physical fermion mass is given by

$$m_f = \left[\hat{m}_f - \frac{1}{2}\hat{B}_L(m_f^2) - \frac{1}{2}\hat{B}_R(m_f^2) \right] \left[1 + \frac{1}{2}\hat{A}_L(m_f^2) + \frac{1}{2}\hat{A}_R(m_f^2) \right]^{-1}, \quad (2.19)$$

while the residue of the pole is

$$\hat{Z}_\psi = \left[1 + \hat{A}_L(m_f^2)P_L + \hat{A}_R(m_f^2)P_R \right]^{-1}. \quad (2.20)$$

The renormalized vertex functions for CC amplitudes are relatively straightforward. We illustrate using the muon decay process $\mu^- \rightarrow \nu_\mu W^-$, for which the tree-level amplitude is

$$i\mathcal{M}_0^{W\mu\nu\mu} = i\frac{g}{\sqrt{2}}\bar{\nu}_\mu \not{W}^+ P_L \mu \quad (2.21)$$

After one-loop renormalization, one has

$$i\mathcal{M}_0^{W\mu\nu\mu} + i\mathcal{M}_{\text{vertex}}^{W\mu\nu\mu} = i\frac{\hat{g}(\mu)}{\sqrt{2}} \left[1 + \hat{F}_V(k^2) - \frac{1}{2} \left\{ \hat{A}_L^\mu(m_\mu^2) + \hat{A}_L^{\nu\mu}(0) \right\} \right] \bar{\nu}_\mu \not{W}^+ P_L \mu \quad (2.22)$$

where $\hat{g}(\mu)$ is the running $SU(2)_L$ gauge coupling and $\hat{F}_V(k^2)$ is the finite part of the one-loop vertex correction.

For processes such as μ -decay and β -decay, one requires the renormalized four-fermion amplitude, $\mathcal{M}_{\text{box}}^{\text{CC}}$. In addition to the vertex and propagator corrections introduced above, $\mathcal{M}_{\text{box}}^{\text{CC}}$ receives additional finite one-loop contributions associated with box graphs involving the exchange of two vector bosons. Since the external fermion masses and momenta for nuclear physics processes are small compared to the weak scale, the box contributions have the form of a product of two left-handed currents, $(V-A) \otimes (V-A)$. In the case of $\mu^- \rightarrow \nu_\mu e^- \bar{\nu}_e$ one has

$$i\mathcal{M}_{\text{box}}^{\text{CC}} = -i\frac{\hat{g}^2}{2\hat{M}_W^2} \hat{\delta}_{\text{box}} \bar{\nu}_\mu \gamma^\lambda P_L \mu \bar{e} \gamma_\lambda P_L \nu_e + \dots, \quad (2.23)$$

where the $+\dots$ indicate terms whose structure differs from the $(V-A) \otimes (V-A)$ structure of the tree-level CC amplitude. In the SM, such terms will be suppressed by factors of m_μ^2/M_W^2 .

Including the box contribution along with the other renormalized one-loop contributions and working in the $k^2 \ll M_W^2$ limit, one obtains the renormalized four fermion amplitude:

$$\begin{aligned} i\mathcal{M}_{\text{tree}}^{\text{CC}} + i\mathcal{M}_{\text{vertex}}^{\text{CC}} + i\mathcal{M}_{\text{propagator}}^{\text{CC}} + i\mathcal{M}_{\text{box}}^{\text{CC}} &= -i\frac{\hat{g}^2}{2\hat{M}_W^2} \left[1 + \frac{\hat{\Pi}_{WW}^T(0)}{\hat{M}_W^2} \right. \\ &- \frac{1}{2} \left\{ \hat{A}_L^\mu(m_\mu^2) + \hat{A}_L^e(m_e^2) + \hat{A}_L^{\nu_e}(0) + \hat{A}_L^{\nu\mu}(0) \right\} + \hat{F}_V^e(0) + \hat{F}_V^\mu(0) + \hat{\delta}_{\text{box}} \left. \right] \\ &\times \bar{\nu}_\mu \gamma^\lambda P_L \mu \bar{e} \gamma_\lambda P_L \nu_e + \dots, \end{aligned} \quad (2.24)$$

or

$$i\mathcal{M}_{\text{one-loop}}^{\text{CC}} = -i\frac{\hat{g}^2}{2\hat{M}_W^2} \left[1 + \frac{\hat{\Pi}_{WW}^T(0)}{\hat{M}_W^2} + \hat{\delta}_{VB} \right] \bar{\nu}_\mu \gamma^\lambda P_L \mu \bar{e} \gamma_\lambda P_L \nu_e + \dots, \quad (2.25)$$

where $\hat{\delta}_{VB}^{(\mu)}$ denotes the fermion propagator, vertex, and box graph contributions.

The example of the muon decay amplitude is particularly important, since the measurement of the muon lifetime provides one of the three required inputs for the SM gauge-Higgs sector. Taking into account the one-loop corrections and including the bremsstrahlung contribution leads to the muon decay rate:

$$\begin{aligned} \frac{1}{\tau_\mu} &= \frac{m_\mu^5}{96\pi^3} \left(\frac{\hat{g}^2}{8\hat{M}_W^2} \right)^2 \left[1 + \frac{\hat{\Pi}_{WW}^T(0)}{\hat{M}_W^2} + \hat{\delta}_{VB}^{(\mu)} \right]^2 + \text{brem} \\ &= \frac{m_\mu^5}{192\pi^3} G_\mu^2 [1 + \delta_{\text{QED}}] \quad , \end{aligned} \quad (2.26)$$

where τ_μ is the muon lifetime and the second equality defines the μ -decay Fermi constant, G_μ , and where

$$\delta_{\text{QED}} = \frac{\alpha}{2\pi} \left(\frac{25}{4} - \pi^2 \right) + \dots \quad (2.27)$$

denotes the contributions from real and virtual photons computed in the Fermi theory of the decay. As a result, one may express the μ -decay Fermi constant in terms of the $\text{SU}(2)_L$ coupling, W -boson mass parameter, and radiative corrections:

$$\frac{G_\mu}{\sqrt{2}} = \frac{\hat{g}^2}{8\hat{M}_W^2} \left[1 + \frac{\hat{\Pi}_{WW}^T(0)}{\hat{M}_W^2} + \hat{\delta}_{VB}^{(\mu)} \right] \equiv \frac{\hat{g}^2}{8\hat{M}_W^2} (1 + \Delta\hat{r}_\mu) \quad , \quad (2.28)$$

where $\hat{\delta}_{VB}^{(\mu)}$ is given by $\hat{\delta}_{VB}$ but with the Fermi theory QED contributions subtracted out.

Along with the fine structure constant and the Z -boson mass, M_Z , the value of G_μ is one of the three most precisely determined parameters in the gauge-Higgs sector of the SM. When computing other electroweak observables, it is conventional to express \hat{g}^2 in terms of G_μ , \hat{M}_W , and the correction $\Delta\hat{r}_\mu$:

$$\hat{g}^2 = \frac{8\hat{M}_W^2 G_\mu}{\sqrt{2}} \frac{1}{1 + \Delta\hat{r}_\mu} \quad . \quad (2.29)$$

To illustrate the use of this expression, consider now the corresponding amplitude for the β -decay $d \rightarrow ue^-\bar{\nu}_e$:

$$i\mathcal{M}_{\beta\text{-decay}} = i \frac{\hat{g}^2}{2\hat{M}_W^2} V_{ud} (1 + \Delta\hat{r}_\beta) \bar{u}\gamma^\lambda P_L d \bar{e}\gamma_\lambda P_L \nu_{\bar{e}} \quad , \quad (2.30)$$

where $\Delta\hat{r}_\beta$ is the analog of $\Delta\hat{r}_\mu$ for the semileptonic four-fermion amplitude but, in contrast with the μ -decay case, also contains virtual photon contributions. Infrared divergences associated with the latter are cancelled by real radiation contributions to the decay rate. Substituting \hat{g}^2 as given in Eq. (2.29) we then obtain

$$i\mathcal{M}_{\beta\text{-decay}} = i \frac{G_\mu}{\sqrt{2}} V_{ud} (1 + \Delta\hat{r}_\beta - \Delta\hat{r}_\mu) \bar{u}\gamma^\lambda (1 - \gamma_5) d \bar{e}\gamma_\lambda (1 - \gamma_5) \nu_{\bar{e}} \quad . \quad (2.31)$$

Importantly, the SM prediction for $\mathcal{M}_{\beta\text{-decay}}$ depends on the difference of the purely leptonic corrections $\Delta\hat{r}_\mu$ and the semileptonic corrections $\Delta\hat{r}_\beta$. Any corrections that are common to both processes, such as corrections to the W -boson propagator or to the first-generation lepton external legs, will cancel in this difference.

Looking ahead to the review of weak decays [19], we alert the reader to some notational differences. In that work one encounters the quantities δ_β , δ_μ , ϵ_L , and ϵ_μ . The correspondence with the foregoing discussion is: $\Delta\hat{r}_{\beta,\mu} \rightarrow \delta_{\beta,\mu}$ while ϵ_L and ϵ_μ denote the corresponding contributions from BSM physics that enter, respectively, like $\Delta\hat{r}_\beta$ and $\Delta\hat{r}_\mu$.

2.4 Neutral Current Processes

Although renormalization of neutral current (NC) amplitudes is similar to that of CC interactions, new aspects arise associated with mixing between the $SU(2)_L$ and $U(1)_Y$ sectors. Among the earliest studies of NC renormalization that addressed these issues are those of Refs. [20, 21, 22, 23]. Here, we highlight three features: the presence of right-handed as well as left-handed fermion fields; the relative normalization of the NC and CC amplitudes encapsulated by an appropriately defined “ ρ -parameter”; and the appearance of the weak mixing angle whose scale-dependence (in the $\overline{\text{MS}}$) arises from loop effects.

To illustrate this added richness, consider the general structure of the renormalized amplitude for the neutral current process $\ell + f \rightarrow \ell + f$ is

$$i\mathcal{M}_{\text{one-loop}}^{\text{NC}} = -i \frac{G_\mu}{2\sqrt{2}} \hat{\rho}_{\text{NC}}(k^2) \frac{M_Z^2}{k^2 - M_Z^2 + iM_Z\Gamma_Z} \bar{\ell} \gamma^\lambda (\hat{g}_V^\ell + \hat{g}_A^\ell \gamma_5) \ell \bar{f} \gamma_\lambda (\hat{g}_V^f + \hat{g}_A^f \gamma_5) f + \text{box}, \quad (2.32)$$

where ℓ and f denote the lepton and fermion spinors, respectively, and “+ box” denotes the box diagram contributions. The quantity $\hat{\rho}_{\text{NC}}$ is a normalization factor common to all four-fermion NC processes that can be expressed in terms of gauge boson masses, the $\hat{\Pi}_{VV}^T(k^2)$, and $\Delta\hat{r}_\mu$ [24]:

$$\hat{\rho}(k^2)_{\text{NC}} = 1 + \frac{\text{Re } \hat{\Pi}_{ZZ}^T(M_Z^2)}{M_Z^2} - \frac{\hat{\Pi}_{WW}^T(0)}{M_W^2} - \frac{\text{Re} \left[\hat{\Pi}_{ZZ}^T(k^2) - \hat{\Pi}_{ZZ}^T(M_Z^2) \right]}{k^2 - M_Z^2} - \hat{\delta}_{VB}^{(\mu)}, \quad (2.33)$$

where

$$M_Z^2 = \hat{M}_Z^2 - \hat{\Pi}_{ZZ}^T(M_Z^2) \quad (2.34)$$

and $M_Z\Gamma_Z = \text{Im } \hat{\Pi}_{ZZ}^T(k^2)$.

The quantities \hat{g}_V^f and \hat{g}_A^f denote the renormalized Z^0 -fermion vector and axial vector couplings, respectively. While their tree-level values depend on the third component of weak isospin (I_3^f) and electric charge (Q_f) of fermion f as well as the weak mixing angle, renormalization introduces an additional dependence on a universal renormalization factor $\hat{\kappa}$, along with process-specific vector and axial vector radiative corrections:

$$\hat{g}_V^f = 2I_3^f - 4\hat{\kappa}(k^2, \mu) \sin^2 \hat{\theta}_W(\mu) Q_f + \hat{\lambda}_V^f \quad (2.35)$$

$$\hat{g}_A^f = -2I_3^f + \hat{\lambda}_A^f. \quad (2.36)$$

Here, $\sin^2 \hat{\theta}_W(\mu) \equiv \hat{s}^2(\mu)$ denotes the weak mixing angle in the $\overline{\text{MS}}$ scheme:

$$\sin^2 \hat{\theta}_W(\mu) = \frac{\hat{g}'(\mu)^2}{\hat{g}(\mu)^2 + \hat{g}'(\mu)^2}; \quad (2.37)$$

and $\hat{\lambda}_{V,A}^f$ are process-dependent corrections that vanish at tree-level. Here \hat{g} and \hat{g}' are the $SU(2)_L$ and $U(1)_Y$ coupling, respectively.

We emphasize that Eq. (2.37) constitutes a definition of the weak mixing angle in the $\overline{\text{MS}}$ scheme and it differs in general from the definition in other schemes. For example, on-shell renormalization (OSR) promotes the tree-level relation $\sin^2 \theta_W = 1 - M_W^2/M_Z^2$ to a definition that holds after renormalization. While the OSR and $\overline{\text{MS}}$ definitions are identical at tree-level, their equality is broken at the one-loop level. Although OSR is often considered more intuitive, it is less conducive for making the most precise SM predictions. In particular, $\sin^2 \hat{\theta}_W(\mu) \equiv \hat{s}^2(M_Z)$ can be obtained from the values of G_μ , α , and M_Z , which are all known with better precision than M_W as is needed for the OSR definition. Using

$$\hat{e}^2(\mu) = \hat{g}^2(\mu) \hat{s}^2(\mu) \quad (2.38)$$

$$\hat{M}_W^2 = \hat{M}_Z^2 \hat{c}^2, \quad (2.39)$$

writing

$$\hat{\alpha}(\mu) = \alpha + \Delta\hat{\alpha}(\mu) \quad (2.40)$$

where α is the fine structure constant, employing Eqs. (2.29,2.34), and choosing $\mu = M_Z$ we obtain

$$\hat{s}^2(M_Z)\hat{c}^2(M_Z) = \frac{\pi\alpha}{\sqrt{2}M_Z^2 G_\mu [1 - \Delta\hat{r}(M_Z)]} \quad (2.41)$$

where

$$\Delta\hat{r}(\mu) = \Delta\hat{r}_\mu + \frac{\Delta\hat{\alpha}}{\alpha} - \frac{\hat{\Pi}_{ZZ}^T(M_Z^2, \mu)}{M_Z^2} \quad (2.42)$$

Looking ahead to the NC review [25], Eqs. (2.41,2.42) correspond to Eq. (35) in that discussion. There one also finds the related quantities Δr for OSR and $\Delta\hat{r}_W$ that is appropriate when using M_W^2 in place of $\hat{c}^2(M_Z)M_Z^2$. A particular advantage of the $\overline{\text{MS}}$ definition of the weak mixing angle is the absence of a quadratic m_t -dependence that enters the OSR definition.

By itself, $\hat{s}^2(\mu)$ is not an observable since it depends on the renormalization scale. One may, however, define an effective weak mixing angle that is μ -independent and that may in principle be isolated experimentally by comparing experiments with different species of fermions:

$$\sin^2 \hat{\theta}_W(k^2)^{\text{eff}} \equiv \hat{\kappa}(k^2, \mu) \sin^2 \hat{\theta}_W(\mu) \quad (2.43)$$

Here the quantity $\hat{\kappa}(k^2, \mu)$ introduced earlier describes a class of electroweak radiative corrections that is independent of the species of fermion involved in the NC interaction. Contributions to $\hat{\kappa}(k^2, \mu)$ arise primarily from the Z - γ mixing tensor:

$$\hat{\Pi}_{Z\gamma}^{\mu\nu}(k^2) = \hat{\Pi}_{Z\gamma}^T(k^2)T^{\mu\nu} + \hat{\Pi}_{Z\gamma}^L(k^2)L^{\mu\nu} \quad (2.44)$$

For processes involving $|k^2| \ll M_Z^2$ that are the focus of this Issue, contributions from light fermions to $\hat{\kappa}(k^2, \mu)$ can lead to the presence of large logarithms when one chooses $\mu = M_Z$. The presence of these logarithms can spoil the expected behavior of the perturbation series unless they are summed to all orders.

To illustrate, consider the amplitude for low-energy, parity-violating Møller scattering:

$$\mathcal{M}_{PV}^{ee} = \frac{G_\mu}{2\sqrt{2}} \hat{\rho}_{\text{NC}}(0) \hat{g}_V^e \hat{g}_A^e \bar{e} \gamma_\mu e \bar{e} \gamma^\mu \gamma_5 e \quad (2.45)$$

with

$$Q_W^e \equiv \hat{\rho}_{\text{NC}}(0) \hat{g}_V^e \hat{g}_A^e = \hat{\rho}_{\text{NC}}(0) \left[-1 + 4\hat{\kappa}(0, \mu) \hat{s}^2(\mu) + \hat{\lambda}_V^f + \hat{\lambda}_A^f (-1 + 4\hat{s}^2) \right] + \dots \quad (2.46)$$

being the ‘‘weak charge’’ of the electron and with the $+\dots$ indicating box diagram contribution and terms of order $(\alpha/4\pi)^2$. At tree-level ($\hat{\kappa} \rightarrow 1$, $\hat{\lambda}_{V,A}^e \rightarrow 0$), the weak charge is suppressed, since \hat{s}^2 is numerically close to 1/4: $Q_W^{e, \text{tree}} \sim -0.1$. Inclusion of one-loop SM radiative corrections reduce the magnitude of Q_W^e by nearly 40 %, owing largely to the near cancellation between the first two terms in Eq. (2.46) and the presence of large logarithms in $\hat{\kappa}(0, \mu)$ when μ is chosen to be M_Z as is conventional[26]. Given these two considerations, one would expect the relative size of two-loop corrections to Q_W^e to be considerably larger than the nominal $\alpha/4\pi$ scale.

In order to improve the convergence of the SM prediction for Q_W^e , one should like to sum the large logarithms to all orders. The use of the running $\sin^2 \hat{\theta}_W(\mu)$ provides a means for doing so. By choosing $\mu \sim Q$ in both $\hat{\kappa}(k^2, \mu)$ and $\sin^2 \hat{\theta}_W(\mu)$, using the requirement that their product is μ -independent as per Eq. (2.43), and solving the RG equations for $\sin^2 \hat{\theta}_W(\mu)$ as in Ref. [27], one effectively moves all the large logarithms from $\hat{\kappa}(k^2, \mu)$ into $\sin^2 \hat{\theta}_W(\mu)$ and sums them to all orders. The result is a SM prediction for $\sin^2 \hat{\theta}_W(k^2)^{\text{eff}}$ with substantially smaller truncation error than would be obtained by the

naive application of perturbation theory to one-loop order. Moreover, as first emphasized in Ref. [26], the SM prediction for $\sin^2 \hat{\theta}_W(k^2)^{\text{eff}}$ provides a useful benchmark against which to compare various NC experimental results. Since $\hat{\kappa}(k^2, Q) - 1$ has its expected magnitude of order α/π , it is also reasonable to use $\sin^2 \hat{\theta}_W(Q)$ for this purpose.

A detailed discussion of the SM prediction for the running of $\hat{s}^2(\mu)$ in the $\overline{\text{MS}}$ will appear in the article on neutral current observables in this Issue (see also Ref. [27]), and we refer the reader to that article for details. Results from the most recent work are shown in Fig. 1 of that article.

Of particular interest for this Issue is the weak mixing angle at $Q = 0$, which takes on the value[27]:

$$\sin^2 \hat{\theta}_W(0) = 0.23867 \pm 0.00016 \quad . \quad (2.47)$$

Note that the error is dominated by the experimental error in $\sin^2 \hat{\theta}_W(M_Z)$ and that the value of $\hat{s}^2(\mu)$ at the two scales differs by roughly three percent. Several present and prospective NC experiments are sensitive to this running, including measurements of the PV asymmetries in Möller scattering, the PV asymmetries in both elastic and inelastic electron-hadron scattering, and atomic PV observables that are insensitive to the nuclear spin. The PV Möller and elastic ep asymmetries are particularly sensitive to $\sin^2 \hat{\theta}_W(0)$, as they depend on $1 - 4\hat{\kappa} \sin^2 \hat{\theta}_W(0) \approx 0.1$. Because of this fortuitous suppression, relatively small changes in $\sin^2 \hat{\theta}_W(0)$ (such as the three percent effect due to running) can lead to considerably larger effects in the asymmetries. Consequently, inclusion of the running effect in the weak mixing angle is vital to the interpretation of these low-energy observables in terms of possible BSM physics.

The corrections contained in the $\hat{\lambda}_{V,A}^f$ contain the Zff vertex and external leg corrections and are specific to the fermion species. A similar remark applies to the box graphs that contribute to the four-fermion amplitudes and that cannot be absorbed into the individual vector and axial vector couplings. An additional contribution to the four fermion amplitudes is generated by γ exchange and involves the so-called anapole coupling of the fermion[28, 29]

$$\mathcal{L}_{\text{anapole}} = \frac{eF_A}{M^2} \bar{\psi} \gamma_\mu \gamma_5 \psi \partial_\nu F^{\mu\nu} \quad , \quad (2.48)$$

where F_A is the dimensionless anapole moment and M is an appropriate mass scale. The interaction $\mathcal{L}_{\text{anapole}}$ generates a contribution to the fermion matrix element of the electromagnetic current:

$$\begin{aligned} \langle p' | J_\mu^{EM}(0) | p \rangle &= \bar{U}(p') \left[F_1 \gamma_\mu + \frac{iF_2}{2M} \sigma_{\mu\nu} k^\nu \right. \\ &\quad \left. + \frac{F_A}{M^2} (k^2 \gamma_\mu - \not{k} k_\mu) \gamma_5 + \frac{iF_E}{2M} \sigma_{\mu\nu} k^\nu \gamma_5 \right] U(p) \quad , \end{aligned} \quad (2.49)$$

where $k = p' - p$ and where F_1 , F_2 , F_A , and F_E give the Dirac, Pauli, anapole, and electric dipole form factors, respectively³. Since only weak interactions can give rise to the parity-odd photon-fermion anapole coupling, we choose $M = M_Z$ in Eq. (2.48). From Eq. (2.48) one sees that the anapole coupling gives rise to a contact interaction in co-ordinate space, since $\partial_\nu F^{\mu\nu} = j_\mu$ with j_μ being the current of the other fermion involved in the low-energy interaction.

We note that the coupling F_A itself depends on the choice of electroweak gauge, and only the complete one-loop scattering amplitude that includes all $\mathcal{O}(\alpha)$ electroweak radiative corrections (including F_A) is gauge-independent (see Ref. [29] and references therein). Nonetheless, when classifying various topologies of the one-loop corrections, it is useful to separate out the anapole contributions that behave like an effective contribution to the product of vector coupling \hat{g}_V^f and the axial vector coupling $\hat{g}_A^{f'}$:

$$\left(\hat{g}_A^{f'} \hat{g}_V^f \right)_{\text{anapole}} = -16\hat{c}^2 \hat{s}^2 Q_f F_A^{f'} \quad . \quad (2.50)$$

³Note that the overall sign of the anapole term in Eq. (2.49) differs from the convention used in Ref. [30].

Adding the anapole contribution to those from the other one-loop corrections leads to a gauge-invariant scattering amplitude. Analogous γ -exchange effects enter in the scattering amplitudes for neutrino scattering from charged particles. In this case, the anapole contribution is equivalent to the neutrino charge radius. In the NC review, the charge radii/anapole, box graph, and vertex plus external leg corrections, and gauge boson propagator corrections are separately discussed, though one should keep in mind this classification carries a gauge-dependence.

When looking beyond the SM radiative corrections to possible loop-induced BSM contributions to low-energy precision NC observables, it is important to include constraints from higher-energy studies. Prior to the operation of the LHC, the most important constraints had been obtained from precision Z -pole observables. In the corresponding theoretical interpretation, it has been useful to characterize possible corrections to the gauge boson propagators from new heavy particles in terms of the so-called oblique parameters, S , T , U [31, 32, 33, 34, 35, 36, 37, 38]:

$$\begin{aligned}
S &= \frac{4\hat{s}^2\hat{c}^2}{\hat{\alpha}M_Z^2} \text{Re} \left\{ \hat{\Pi}_{ZZ}(0) - \hat{\Pi}_{ZZ}(M_Z^2) + \frac{\hat{c}^2 - \hat{s}^2}{\hat{c}\hat{s}} \left[\hat{\Pi}_{Z\gamma}(M_Z^2) - \hat{\Pi}_{Z\gamma}(0) \right] + \hat{\Pi}_{\gamma\gamma}(M_Z^2) \right\}^{\text{New}}, \\
T &= \frac{1}{\hat{\alpha}M_W^2} \left\{ \hat{c}^2 \left(\hat{\Pi}_{ZZ}(0) + \frac{2\hat{s}}{\hat{c}} \hat{\Pi}_{Z\gamma}(0) \right) - \hat{\Pi}_{WW}(0) \right\}^{\text{New}}, \\
U &= \frac{4\hat{s}^2}{\hat{\alpha}} \left\{ \frac{\hat{\Pi}_{WW}(0) - \hat{\Pi}_{WW}(M_W^2)}{M_W^2} + \hat{c}^2 \frac{\hat{\Pi}_{ZZ}(M_Z^2) - \hat{\Pi}_{ZZ}(0)}{M_Z^2} \right. \\
&\quad \left. + 2\hat{c}\hat{s} \frac{\hat{\Pi}_{Z\gamma}(M_Z^2) - \hat{\Pi}_{Z\gamma}(0)}{M_Z^2} + \hat{s}^2 \frac{\hat{\Pi}_{\gamma\gamma}(M_Z^2)}{M_Z^2} \right\}^{\text{New}}, \tag{2.51}
\end{aligned}$$

where the superscript ‘‘New’’ indicates that only the new physics contributions to the self-energies are included. Contributions to gauge-boson self energies can be expressed entirely in terms of the oblique parameters S , T , and U in the limit that $\Lambda \gg M_Z$.

Expressing BSM loop contributions to $\hat{\rho}$ and $\sin^2 \hat{\theta}_W(k^2)^{\text{eff}} = \hat{\kappa}(k^2, \mu) \sin^2 \hat{\theta}_W(\mu)$ in terms of S, T , and U we obtain:

$$\begin{aligned}
\delta \hat{\rho}^{\text{BSM loop}} &= \hat{\alpha}T - \hat{\delta}_{VB}^\mu, \\
\left(\frac{\delta \sin^2 \hat{\theta}_W^{\text{eff}}}{\sin^2 \hat{\theta}_W^{\text{eff}}} \right)^{\text{BSM loop}} &= \left(\frac{\hat{c}^2}{\hat{c}^2 - \hat{s}^2} \right) \left(\frac{\hat{\alpha}}{4\hat{s}^2\hat{c}^2} S - \hat{\alpha}T + \hat{\delta}_{VB}^\mu \right) + \frac{\hat{c}}{\hat{s}} \left[\frac{\hat{\Pi}_{Z\gamma}(k^2)}{k^2} - \frac{\hat{\Pi}_{Z\gamma}(M_Z^2)}{M_Z^2} \right] \\
&\quad + \left(\frac{\hat{c}^2}{\hat{c}^2 - \hat{s}^2} \right) \left[-\frac{\hat{\Pi}_{\gamma\gamma}(M_Z^2)}{M_Z^2} + \frac{\Delta\hat{\alpha}}{\alpha} \right], \tag{2.52}
\end{aligned}$$

where k^2 is the typical momentum transfer for a given process. For low energy interactions, $k^2 \rightarrow 0$. Note that we have included in $\delta \sin^2 \hat{\theta}_W^{\text{eff}}$ both the contribution from $\hat{\Pi}_{Z\gamma}(k^2)/k^2$ that enters $\hat{\kappa}(k^2, \mu)$ as well as the shift in $\hat{s}^2(M_Z^2)$ obtained from Eq. (2.41) as discussed above. Eqs. (2.52) provide a useful means of incorporating Z^0 -pole constraints on BSM loop effects. For example, $\delta \hat{\rho}^{\text{BSM loop}}$ is highly constrained by bounds on T obtained from such observables. In contrast, $[\delta \sin^2 \hat{\theta}_W(k^2)^{\text{eff}}]^{\text{BSM loop}}$ is less stringently constrained.

2.5 Theoretical Uncertainties in Electroweak Radiative Corrections

An important consideration in exploiting low-energy, precision electroweak observables as a probe of BSM physics is to ensure that the theoretical uncertainties associated with SM contributions are well-

below the level of possible BSM effects. The SM uncertainties generally involve one of two considerations: (i) neglect of higher order electroweak contributions, and (ii) contributions from strong interactions. We have already touched on the latter in our short discussion of $g_\mu - 2$. While an extensive discussion of these considerations goes beyond the scope of the present article, we give here a brief overview of the strategies employed to address them.

Nominally, one expects the one-loop contributions to quantities such as $\Delta\hat{r}_\mu$, $\hat{\kappa}$, *etc.* to be of order $\alpha/\pi \sim 10^{-3}$, so that neglect of two- and higher-loop effects is well justified for the present level of experimental sensitivity. Moreover, since SUSY loop contributions must generally decouple in the $\Lambda \rightarrow \infty$ limit, one expects the relative magnitude of their contributions to be

$$\delta_{\text{BSM loop}} = \frac{\delta\mathcal{O}^{\text{BSM loop}}}{\mathcal{O}^{\text{SM}}} \sim \frac{\alpha}{\pi} \left(\frac{M}{\Lambda}\right)^2, \quad (2.53)$$

where M is the relevant SM mass. For low-energy electroweak processes, one has $M \rightarrow v$, so that for $\Lambda \gtrsim v$ one expects $\delta_{\text{BSM loop}}$ to be somewhat smaller than, the scale of one-loop, SM electroweak corrections. From this standpoint, neglect of two-loop SM contributions is a justifiable approximation. As discussed above, however, exceptions may occur when the one-loop SM contributions contain large logarithms (as in the case of $\hat{\kappa}$), when the tree-level SM amplitudes are suppressed (*e.g.*, NC amplitudes proportional to \hat{g}_V^c), or both. In such situations, the summing terms of the form $\alpha^n \ln^n(\mu/\mu_0)$ is essential, and the RG equations can be employed for this purpose.

Reduction of theoretical uncertainties associated with QCD corrections is generally more challenging. Short-distance QCD contributions can be treated using the operator product expansion (OPE), and the resulting correction to a given order in α_s achieved with sufficient effort. In the case of PV electron-proton scattering, for example, the one-loop WW box contribution is anomalously – but not logarithmically – enhanced, and its contribution to the proton weak charge, Q_W^p , nearly cancels that of the large logarithms appearing in $\hat{\kappa}$ [or resummed into $\sin^2\hat{\theta}_W(0)$]. Since the semileptonic, WW box graphs involve hadronic intermediate states one could expect relatively important QCD corrections to the one-loop amplitude. Because the loop integral is dominated by high momentum scales the corrections can be computed using the OPE, leading to [39]

$$\delta Q_W^p(WW \text{ box}) = \frac{\hat{\alpha}}{4\pi\hat{s}^2} \left[2 + 5 \left(1 - \frac{\alpha_s(M_W)}{\pi} \right) \right] \quad (2.54)$$

for a total QCD correction of $\approx -0.7\%$.

A more problematic situation arises for one-loop corrections that sample momenta of order the hadronic scale. To illustrate, we first consider PV electron scattering. For both PV Møller and elastic ep scattering, light quark loop contributions to $\hat{\Pi}_{Z\gamma}^T$ lead to hadronic uncertainties in $\hat{\kappa}(0, \mu)$. Traditionally, light quark contributions have been computed by relating $\hat{\Pi}_{Z\gamma}^T$ to the $\sigma(e^+e^- \rightarrow \text{hadrons})$ via dispersion relations[21, 23], much as one does in computing hadronic vacuum polarization contributions to a_μ . In the case of $\hat{\Pi}_{Z\gamma}^T$, however, additional assumptions regarding flavor symmetry in the current-current correlator are needed in order to make use of e^+e^- data. Recently, these assumptions have been examined and more stringent bounds on the hadronic uncertainty in $\hat{\kappa}(0, \mu)$ obtained[27].

For semileptonic processes, additional hadronic uncertainties appear in box graphs that contain one γ and one weak gauge boson. In contrast to the situation for the WW -box graphs, the γZ loop integral samples all momentum from the hadronic scale to the weak scale. Neglecting the short-distance, perturbative QCD corrections, one finds

$$\delta Q_W^p(\gamma Z \text{ box}) = \frac{5\hat{\alpha}}{2\pi} (1 - 4\hat{s}^2) \left[\ln \left(\frac{M_Z^2}{\Lambda_H^2} \right) + C_{\gamma Z}(\Lambda_H) \right], \quad (2.55)$$

where the hadronic scale Λ_H is a scale characterizing the transition between the perturbative and non-perturbative domains⁴ and $C_{\gamma Z}(\Lambda_H)$ parameterizes contributions to the loop integral from momenta $\sqrt{|k^2|} \lesssim \Lambda_H$. The coefficient of logarithm in Eq. (2.55) is determined by short distance dynamics and can be calculated reliably in perturbation theory. However, the value of $C_{\gamma Z}(\Lambda_H)$ is sensitive to long-distance scales and has not, as yet, been computed from first principles in QCD. A similar contribution arises in neutron, nuclear, and pion β -decay. An estimate of the theoretical uncertainty associated with these contributions had been made by varying Λ over the range $400 \leq \Lambda_H \leq 1600$ MeV. The corresponding variation in the logarithmic term in Eq. (2.55) was used as an indication of the uncertainty associated with long-distance contributions to the box graph integral. Recently, Marciano and Sirlin observed that for the γW box, both the pQCD corrections to the logarithmic term as well as the value of Λ_H could be obtained by comparison with the theoretical expression for the Bjorken Sum Rule using isospin symmetry[17]. As a result, these authors have reduced the previously-quoted theoretical error by a factor of two. The analogous treatment of the γZ box is more complex, since one cannot obtain the isoscalar contribution from isospin arguments. In both cases, the more refined estimates of the uncertainty associated with the low-energy constants $C_{\gamma Z}$ and $C_{\gamma W}$ remain to be performed.

For PV electron scattering, there exists an additional contribution to the PV asymmetry associated with the energy-dependence of the γZ box graphs. As an energy-dependent effect, this contribution is not formally part of the fundamental, renormalized electroweak couplings, but rather more akin to a form factor. Nonetheless, the contribution can introduce an additional source of theoretical uncertainty into the extraction of the fundamental couplings from the asymmetry. Consequently, reducing this uncertainty constitutes one of the on-going theoretical challenges for the interpretation of the PV electron scattering experiments. A detailed discussion of this correction and its quantitative impact on the interpretation of the asymmetry measurements can be found in the NC article in this issue as well as in Ref. [10].

3 Beyond the Standard Model

3.1 *Effective Theory Description: generalities*

While the SM successfully describes a wealth of data over a wide range of energies (from atomic scales to hundreds of GeV), both purely theoretical arguments and observed facts about our Universe point to the existence of new degrees of freedom and interactions beyond the SM. With the theoretical bias that new physics originates at high scales (or short distances), we can think of the SM as the low-energy limit of a more fundamental theory.⁵

In this context and in the absence of an emerging “New Standard Model”, it is convenient to describe the dynamics below the scale Λ (at which new particles appear) through an effective field theory (EFT), in which the new heavy particles are “integrated out” and affect the dynamics through a series of higher dimensional operators constructed with the low-energy SM fields. The basic ideas of this approach are illustrated in Fig. 1, which shows the relevant scales involved in the problem and how short-distance physics beyond the SM works its way into low-energy probes:

- Above the scale Λ , where the new particles live, the dynamics is described by the full UV completion of the SM, characterized by a Lagrangian density \mathcal{L}_{BSM} .

⁴This scale is denoted elsewhere in this Issues as the scale of chiral symmetry-breaking, Λ_χ .

⁵Strictly speaking, this way of thinking does not apply to SM extensions that involve light new particles very weakly coupled to the SM.

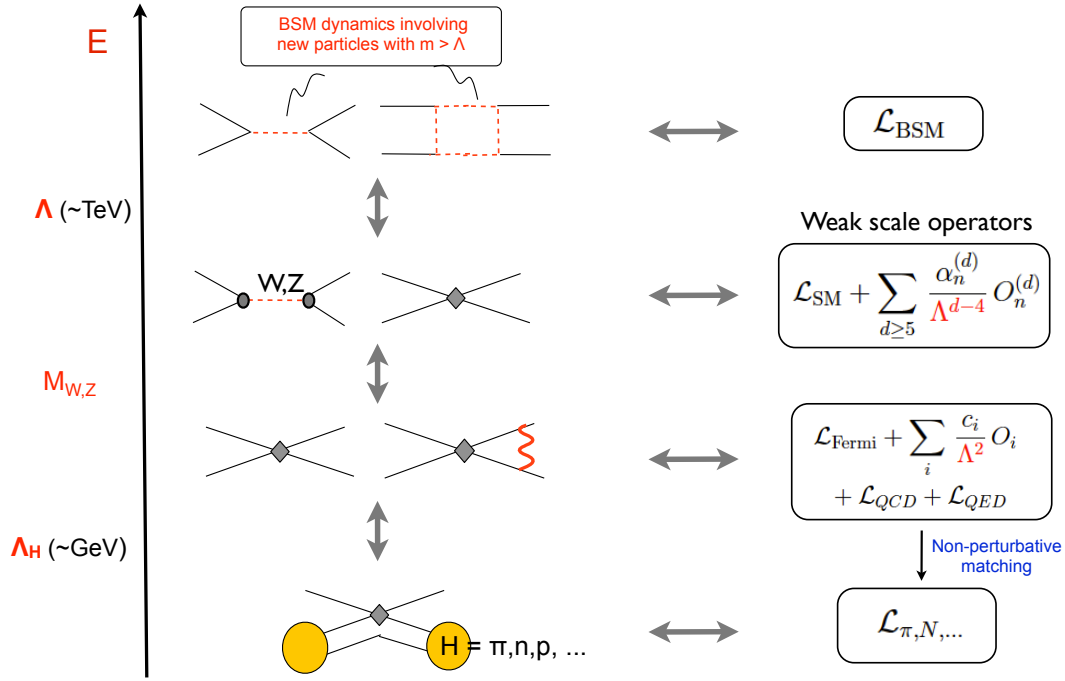


Figure 1: Schematic representation of the series of effective field theories (EFTs) needed to describe the influence of new physics beyond the Standard Model on low-energy observables (see text for details).

- Below the scale Λ , one can “integrate out” the new degrees of freedom. The effective Lagrangian relevant at scales $\Lambda > E > M_{Z,W}$, is the SM Lagrangian augmented by a string of $d > 4$ operators constructed with the low-energy SM fields, suppressed by Λ^{d-4} . Any UV model analysis can be cast in this language through a matching calculation at the scale Λ , which relates the effective couplings to the couplings and masses of the model. The prototypical example of such a matching calculation is the relation between the Fermi constant and the W boson mass and $SU(2)$ gauge coupling of the SM.
- Below the electroweak scale one integrates out W and Z , and the dynamics at $M_{Z,W} > E > \Lambda_H$ (where $\Lambda_H \sim 1$ GeV) is described by a modified set of effective operators (BSM plus electroweak), plus QCD and QED. This picture still involves quarks and gluons as explicit degrees of freedom.
- Finally, to describe processes involving hadrons and nuclei at $E \leq \Lambda_H$, one has to go from a picture of quarks and gluons to a picture of free or bound hadrons. This requires non-perturbative matching calculations. The step from quarks to hadrons exploits the symmetries of QCD and when symmetries are not sufficient typically requires a combination of lattice QCD and Chiral Perturbation Theory (ChPT). The description of nuclei requires the use of non-perturbative non-relativistic many-body techniques.

From the above quick overview both the benefits and limitations of the EFT description should be clear. First, the EFT approach is quite general and allows one to study the implications of low-energy measurements on a large class of models. In particular, note that the operator analysis is certainly

applicable to describe the low-energy probes we are mostly concerned in this review. This method enables us to assess in a model-independent way the possible correlations, relative significance, and impact of various low-energy probes (i.e. those observables sensitive to the same set of BSM effective couplings and operators). Moreover, if the new physics scale Λ is in the multi-TeV region or above (which is an open question), even at LHC energy scales $E \sim 1$ TeV the BSM dynamics can be described in terms of effective operators. In other words, if new physics originates at very high energy ($E > \text{few TeV}$), the operator analysis can be used to directly compare low-energy versus collider probes.

Explicit model analyses are related to the EFT description by matching calculations at the scale Λ . The matching conditions express the effective couplings in terms of the fewer model couplings and masses, implying specific model correlations among the various low-energy couplings (and observables) and the collider phenomenology. In general such correlations are not “visible” in a pure bottom-up EFT approach. In this set of reviews we will use both a general EFT description of low-energy probes and explicit UV models.

3.2 *BSM effective lagrangian*

In this subsection we provide some details on the BSM effective Lagrangian at the TeV scale. This BSM effective Lagrangian provides the starting point for low-energy analyses of various types of probes (CP violation and EDMs, lepton flavor violation, non-standard CC weak interactions, etc), which will be discussed in each individual chapter.

As discussed earlier, given the successes of the SM at energies up to the electroweak scale $v \sim 200$ GeV, we adopt here the point of view that the SM is the low-energy limit of a more fundamental theory. Writing down the effective theory requires specifying (i) a power counting in ratio of scales; (ii) the low-energy degrees of freedom (field content); and (iii) the symmetries respected by the underlying physics. Each of these points comes with some assumptions about the underlying dynamics, which we now briefly discuss:

- **Power counting:** we assume that there is a gap between the weak scale v and the scale Λ where new degrees of freedom appear, We organize the expansion in dimensionality of the new physics operators, whose coefficients scale with inverse powers of Λ , namely $1/\Lambda^{d-4}$. To a given order in v/Λ the EFT is “renormalizable”, in the sense that all the ultraviolet divergences can be reabsorbed in a finite number of parameters.
- **Degrees of freedom:** we need to specify the building blocks of the effective theory. Our default assumptions will be that the low-energy field content is the same as in the SM. Overall, this is a safe assumption, except for two cases, in which this becomes a model assumption and deserves further discussion. (1) Neutrino field content: by making the SM field choice, we assume that there are no light right-handed neutrino fields, sterile with respect to the SM gauge group. This excludes a Dirac-type mass term for neutrinos but at the moment there is no experimental evidence to support this choice. So in some applications to be discussed below we will extend the field content to include ν_R in the low-energy theory. (2) By including the SM Higgs doublet in the low-energy theory, we are making a strong assumption about the mechanism of EWSB. While we know that EW symmetry is broken and the Higgs mechanism is at work (the Goldstone modes become the longitudinal components of the massive gauge bosons), we do not conclusively know how this is realized. By including the SM Higgs in the low-energy theory, we assume that the EWSB sector is weakly coupled and EWSB proceeds as in the SM. This scenario is receiving growing support by the LHC data on the Higgs. The possibility of a Higgs-less effective theory, corresponding to a strongly interacting EWSB sector, looks less likely right now and for simplicity we will not discuss it in detail in this review. EFT analyses in this context can be found in [40, 41, 42, 43].

- Symmetries: one needs to specify the symmetries obeyed by the underlying theory. Here again we will make the standard assumptions of Lorentz invariance and invariance under the gauge SM group (as part of a possibly broader set of underlying symmetries). So the operators induced by the underlying theory will be Lorentz-invariant structures symmetric under $SU(3)_C \times SU(2)_L \times U(1)_Y$. In particular, we do not impose any of the global “accidental” symmetries of the SM, such as baryon number, lepton number, and lepton flavor.⁶

Given the above discussion, one can describe physics at the weak scale (and below) by means of an effective non-renormalizable lagrangian of the form:

$$\mathcal{L}^{(\text{eff})} = \mathcal{L}_{\text{SM}} + \mathcal{L}_5 + \mathcal{L}_6 + \dots \quad (3.56)$$

$$\mathcal{L}_d = \sum_i \frac{\alpha_i^{(d)}}{\Lambda^{d-4}} Q_i^{(d)} , \quad (3.57)$$

where Λ is the scale of the new physics associated with local $SU(2)_L \times U(1)_Y$ gauge-invariant operators $Q_i^{(n)}$ of dimension d built out of SM fields and where the Wilson coefficients $\alpha_i^{(d)}$ embody the details of the underlying dynamics at the energy scale Λ . For example, Λ may denote the mass scale of new degrees of freedom that become active at the BSM energy scale, while the $\alpha_i^{(d)}$ may contain loop factors, couplings, and/or other factors associated with a particular symmetry violation such as CP-violating phases.

Experiments at the intensity / precision frontier typically probe the scale associated with the new operators and their symmetry structure. The operators themselves can be divided in two classes: (i) those that produce corrections to SM allowed processes, and can thus be probed via precision tests; (ii) those that violate exact or approximate SM symmetries and hence mediate forbidden or rare processes. Below, we organize our discussion by increasing dimensionality of the operators.

3.3 Dimension five

At dimension five, only one operator arises [44]. It violates total lepton number and after EWSB generates a Majorana mass term for neutrinos:

$$\mathcal{L}_{\text{Majorana}}^\nu = -\tilde{Y}_\nu^{jk} \frac{1}{\Lambda} (\ell_j)^T C \epsilon \varphi \varphi \ell_k . \quad (3.58)$$

For $v = 246$ GeV, the couplings \tilde{Y}_ν in Eq. (3.58) can be $\mathcal{O}(1)$ if $\Lambda \gtrsim 10^{14}$ GeV. The well-known Seesaw mechanism for neutrino mass generates the Majorana mass term by introducing additional heavy Majorana neutrino fields N_R that couple to the left-handed SM doublets ℓ through interactions of the type (2.13) with the replacement $\nu_R \rightarrow N_R$. When one integrates the N_R out of the low energy effective theory, one obtains (3.58) with $\Lambda = m_{N_R}$. While the N_R could not be directly observed due to their large mass, the existence of the Majorana mass term could provide indirect evidence for their existence. As discussed in detail in the article on lepton flavor and number violation, the observation of the lepton-number violating $0\nu\beta\beta$ process would imply the presence of non-vanishing Majorana couplings \tilde{Y}_ν .

It is remarkable that the first evidence for BSM physics (neutrino mass) can be accounted by the lowest-dimensional effective operator that one can write down.

⁶These symmetries are not imposed on the SM Lagrangian: but it turns out that all the gauge-invariant operators of dimension less than or equal to four respect those symmetries, hence the characterization “accidental”.

X^3		φ^6 and $\varphi^4 D^2$		$\psi^2 \varphi^3$	
Q_G	$f^{ABC} G_\mu^{A\nu} G_\nu^{B\rho} G_\rho^{C\mu}$	Q_φ	$(\varphi^\dagger \varphi)^3$	$Q_{e\varphi}$	$(\varphi^\dagger \varphi)(\bar{l}_p e_r \varphi)$
$Q_{\tilde{G}}$	$f^{ABC} \tilde{G}_\mu^{A\nu} G_\nu^{B\rho} G_\rho^{C\mu}$	$Q_{\varphi\Box}$	$(\varphi^\dagger \varphi)\Box(\varphi^\dagger \varphi)$	$Q_{u\varphi}$	$(\varphi^\dagger \varphi)(\bar{q}_p u_r \tilde{\varphi})$
Q_W	$\varepsilon^{IJK} W_\mu^{I\nu} W_\nu^{J\rho} W_\rho^{K\mu}$	$Q_{\varphi D}$	$(\varphi^\dagger D^\mu \varphi)^* (\varphi^\dagger D_\mu \varphi)$	$Q_{d\varphi}$	$(\varphi^\dagger \varphi)(\bar{q}_p d_r \varphi)$
$Q_{\tilde{W}}$	$\varepsilon^{IJK} \tilde{W}_\mu^{I\nu} W_\nu^{J\rho} W_\rho^{K\mu}$				
$X^2 \varphi^2$		$\psi^2 X \varphi$		$\psi^2 \varphi^2 D$	
$Q_{\varphi G}$	$\varphi^\dagger \varphi G_{\mu\nu}^A G^{A\mu\nu}$	Q_{eW}	$(\bar{l}_p \sigma^{\mu\nu} e_r) \tau^I \varphi W_{\mu\nu}^I$	$Q_{\varphi l}^{(1)}$	$(\varphi^\dagger i \overleftrightarrow{D}_\mu \varphi)(\bar{l}_p \gamma^\mu l_r)$
$Q_{\varphi \tilde{G}}$	$\varphi^\dagger \varphi \tilde{G}_{\mu\nu}^A G^{A\mu\nu}$	Q_{eB}	$(\bar{l}_p \sigma^{\mu\nu} e_r) \varphi B_{\mu\nu}$	$Q_{\varphi l}^{(3)}$	$(\varphi^\dagger i \overleftrightarrow{D}_\mu^I \varphi)(\bar{l}_p \tau^I \gamma^\mu l_r)$
$Q_{\varphi W}$	$\varphi^\dagger \varphi W_{\mu\nu}^I W^{I\mu\nu}$	Q_{uG}	$(\bar{q}_p \sigma^{\mu\nu} T^A u_r) \tilde{\varphi} G_{\mu\nu}^A$	$Q_{\varphi e}$	$(\varphi^\dagger i \overleftrightarrow{D}_\mu \varphi)(\bar{e}_p \gamma^\mu e_r)$
$Q_{\varphi \tilde{W}}$	$\varphi^\dagger \varphi \tilde{W}_{\mu\nu}^I W^{I\mu\nu}$	Q_{uW}	$(\bar{q}_p \sigma^{\mu\nu} u_r) \tau^I \tilde{\varphi} W_{\mu\nu}^I$	$Q_{\varphi q}^{(1)}$	$(\varphi^\dagger i \overleftrightarrow{D}_\mu \varphi)(\bar{q}_p \gamma^\mu q_r)$
$Q_{\varphi B}$	$\varphi^\dagger \varphi B_{\mu\nu} B^{\mu\nu}$	Q_{uB}	$(\bar{q}_p \sigma^{\mu\nu} u_r) \tilde{\varphi} B_{\mu\nu}$	$Q_{\varphi q}^{(3)}$	$(\varphi^\dagger i \overleftrightarrow{D}_\mu^I \varphi)(\bar{q}_p \tau^I \gamma^\mu q_r)$
$Q_{\varphi \tilde{B}}$	$\varphi^\dagger \varphi \tilde{B}_{\mu\nu} B^{\mu\nu}$	Q_{dG}	$(\bar{q}_p \sigma^{\mu\nu} T^A d_r) \varphi G_{\mu\nu}^A$	$Q_{\varphi u}$	$(\varphi^\dagger i \overleftrightarrow{D}_\mu \varphi)(\bar{u}_p \gamma^\mu u_r)$
$Q_{\varphi WB}$	$\varphi^\dagger \tau^I \varphi W_{\mu\nu}^I B^{\mu\nu}$	Q_{dW}	$(\bar{q}_p \sigma^{\mu\nu} d_r) \tau^I \varphi W_{\mu\nu}^I$	$Q_{\varphi d}$	$(\varphi^\dagger i \overleftrightarrow{D}_\mu \varphi)(\bar{d}_p \gamma^\mu d_r)$
$Q_{\varphi \tilde{W}B}$	$\varphi^\dagger \tau^I \varphi \tilde{W}_{\mu\nu}^I B^{\mu\nu}$	Q_{dB}	$(\bar{q}_p \sigma^{\mu\nu} d_r) \varphi B_{\mu\nu}$	$Q_{\varphi ud}$	$i(\tilde{\varphi}^\dagger D_\mu \varphi)(\bar{u}_p \gamma^\mu d_r)$

Table 1: Dimension-six operators other than the four-fermion ones [45]. Following Ref. [45], we adopt the notation $\varphi^\dagger i \overleftrightarrow{D}_\mu \varphi \equiv i\varphi^\dagger (D_\mu - \overleftarrow{D}_\mu) \varphi$, $\varphi^\dagger i \overleftrightarrow{D}_\mu^I \varphi \equiv i\varphi^\dagger (\tau^I D_\mu - \overleftarrow{D}_\mu \tau^I) \varphi$, and $\tilde{\varphi} = \varepsilon\varphi^*$, where $\varepsilon = i\sigma_2$. Generation indices p, r are explicitly displayed for all fermion fields. The operator names in the left column of each block should be supplemented with generation indices of the fermion fields whenever necessary, e.g., $Q_{eW} \rightarrow Q_{eW}^{pr}$. Dirac, color, and weak isospin indices are always contracted within the brackets, and not displayed.

3.4 Dimension six

Dimension six operators violating baryon number were first discussed in [44, 46]. A first systematic classification of all dimension-six operators was given in Ref. [47]. This issue was recently revisited by the authors of Ref. [45], who pointed out some redundancies in the classification of [47]. All in all, barring flavor structures and Hermitian conjugation, the effective Lagrangian contains fifty-nine independent dimension six B-conserving operators: fifteen do not contain any fermion fields, nineteen contain two fermion fields, and twenty-five contain four fermion fields. [45]. Similarly, there are five independent dimension-six operators that violate baryon number. All the dimension-six operators are reported in Tables 1 and 2, taken from Ref. [45]. Note that generation indices p, r, s, t are explicitly displayed for all fermion fields. The bosonic operators are all Hermitian. For the operators containing fermions, Hermitian conjugation is equivalent to transposition of generation indices in each of the fermionic currents in classes $(\bar{L}L)(\bar{L}L)$, $(\bar{R}R)(\bar{R}R)$, $(\bar{L}L)(\bar{R}R)$, and $\psi^2 \varphi^2 D^2$ (except for $Q_{\varphi ud}$). For the remaining operators with fermions, Hermitian conjugates are not listed explicitly.

The B-conserving operators can be organized into three broad categories:

- Operators that do not involve fermions: they mainly modify couplings and properties of the gauge bosons (classes X^3 , $\varphi^4 D^2$, $X^2 \varphi^2$) and may affect reactions involving the physical Higgs boson.
- Operators that involve two fermion fields: after EWSB these induce corrections to the fermion

mass matrices (class $\psi^2\varphi^3$), dipole moments (both CP conserving and violating) of the fermions (class $\psi^2 X\varphi$), and corrections to the gauge-fermion couplings (class $\psi^2\varphi^2 D$, through gauge bosons in the covariant derivatives).

- Four-fermion operators: these induce corrections to purely hadronic processes (four quarks), purely leptonic processes (four leptons), and semi-leptonic processes (both charged- and neutral-current).

It is useful to recall here the properties of the various operators under CP transformation. The bosonic operators containing $\tilde{X}_{\mu\nu}$ are CP-odd, while the remaining ones are CP-even. For a given fermionic operator Q , the combinations $Q \mp Q^\dagger$ is CP-odd (-even). Therefore CP violation requires a non-vanishing imaginary part of the corresponding Wilson coefficient, when the operator is expressed in the mass-eigenstate basis.

Finally, note that both two- and four-fermion operators can mediate flavor-changing neutral current (FCNC) processes in both the lepton and quark sector. Within the SM quark sector FCNCs are suppressed (arise only at loop level), while leptonic FCNC are forbidden (lepton flavor is a good quantum number). Even after minimally extending the SM to include neutrino masses, leptonic FCNC amplitudes are suppressed by the ratio $\Delta m_\nu^2/M_W^2$, making lepton flavor violating (LFV) decays a very promising probe of BSM dynamics.

It is sometimes useful to define effective scales Λ_i that absorb the Wilson coefficients. In the case of dimension-six operators one has:

$$\frac{1}{\Lambda_i^2} \approx \frac{\alpha_i^{(6)}}{\Lambda^2} \quad , \quad (3.59)$$

and similar definitions apply to the scale of operators of any dimensionality. Bounds on the effective scale Λ_i of the dimension-5 and dimension-6 operators can be obtained from a variety of low-energy and collider tests. These will be reviewed in detail in each of the chapters of this issue. Here we provide a first orientation, summarizing the current and prospective bounds in Figure 2.

The effective scales Λ_i that are indicated Fig. 2 may be considered as the maximal scale probed by a given observable. For example, the bounds $\Lambda_{FCNC,CP} > 10^4$ TeV could be reconciled with TeV scale new particles, provided the new dynamics has approximate flavor (or CP) symmetries. Nevertheless, the effective scale Λ_i is a good measure of how deeply a given measurement is constraining the new physics: a large Λ_i is either pushing the mass scale to large values or is telling us something deep about the symmetry structure of the TeV-scale BSM dynamics. With these caveats in mind, Fig. 2 illustrates that the rare / forbidden processes provide the strongest bounds on the effective scale, with $\Lambda_B \sim 10^{16}$ GeV and $\Lambda_L \sim 10^{14}$ GeV. CP violation (EDMs and flavor sector) and FCNC in both the quark and lepton sector provide the next strongest bounds on the effective scale, namely $\Lambda_{CP}, \Lambda_{FCNC} \sim 10^{4-5}$ TeV. Precision measurements such as the muon $g - 2$ and $\pi \rightarrow e\nu$ provide constraints at the level of $\Lambda \sim 100$ TeV, while other charged-current and neutral-current probes are at the level of $\Lambda \sim 10$ TeV. The reach of all these probes overlaps with the LHC reach, so they will provide useful information to reconstruct possible new TeV-scale dynamics that might emerge at the LHC.

3.5 Higher dimensional operators

While most observables receive the leading BSM contribution from dimension-six operators, in some case it is necessary to go beyond dimension six. For example, the leading contributions to Majorana neutrino transition magnetic moments arises from dimension-seven operators [48]. A different example requiring the need for higher dimensional operators involves the study of non-standard flavor-changing neutrino-matter interactions. The dimension-six contributions to these processes are highly suppressed because they are related by SU(2) gauge invariance to the corresponding charged LFV processes. This connection is lost at dimension eight, because it is possible to construct operators that contribute to neutrino-matter FCNC but not to charged LFV [49].

$(\bar{L}L)(\bar{L}L)$		$(\bar{R}R)(\bar{R}R)$		$(\bar{L}L)(\bar{R}R)$	
Q_{ll}	$(\bar{l}_p \gamma_\mu l_r)(\bar{l}_s \gamma^\mu l_t)$	Q_{ee}	$(\bar{e}_p \gamma_\mu e_r)(\bar{e}_s \gamma^\mu e_t)$	Q_{le}	$(\bar{l}_p \gamma_\mu l_r)(\bar{e}_s \gamma^\mu e_t)$
$Q_{qq}^{(1)}$	$(\bar{q}_p \gamma_\mu q_r)(\bar{q}_s \gamma^\mu q_t)$	Q_{uu}	$(\bar{u}_p \gamma_\mu u_r)(\bar{u}_s \gamma^\mu u_t)$	Q_{lu}	$(\bar{l}_p \gamma_\mu l_r)(\bar{u}_s \gamma^\mu u_t)$
$Q_{qq}^{(3)}$	$(\bar{q}_p \gamma_\mu \tau^I q_r)(\bar{q}_s \gamma^\mu \tau^I q_t)$	Q_{dd}	$(\bar{d}_p \gamma_\mu d_r)(\bar{d}_s \gamma^\mu d_t)$	Q_{ld}	$(\bar{l}_p \gamma_\mu l_r)(\bar{d}_s \gamma^\mu d_t)$
$Q_{lq}^{(1)}$	$(\bar{l}_p \gamma_\mu l_r)(\bar{q}_s \gamma^\mu q_t)$	Q_{eu}	$(\bar{e}_p \gamma_\mu e_r)(\bar{u}_s \gamma^\mu u_t)$	Q_{qe}	$(\bar{q}_p \gamma_\mu q_r)(\bar{e}_s \gamma^\mu e_t)$
$Q_{lq}^{(3)}$	$(\bar{l}_p \gamma_\mu \tau^I l_r)(\bar{q}_s \gamma^\mu \tau^I q_t)$	Q_{ed}	$(\bar{e}_p \gamma_\mu e_r)(\bar{d}_s \gamma^\mu d_t)$	$Q_{qu}^{(1)}$	$(\bar{q}_p \gamma_\mu q_r)(\bar{u}_s \gamma^\mu u_t)$
		$Q_{ud}^{(1)}$	$(\bar{u}_p \gamma_\mu u_r)(\bar{d}_s \gamma^\mu d_t)$	$Q_{qu}^{(8)}$	$(\bar{q}_p \gamma_\mu T^A q_r)(\bar{u}_s \gamma^\mu T^A u_t)$
		$Q_{ud}^{(8)}$	$(\bar{u}_p \gamma_\mu T^A u_r)(\bar{d}_s \gamma^\mu T^A d_t)$	$Q_{qd}^{(1)}$	$(\bar{q}_p \gamma_\mu q_r)(\bar{d}_s \gamma^\mu d_t)$
				$Q_{qd}^{(8)}$	$(\bar{q}_p \gamma_\mu T^A q_r)(\bar{d}_s \gamma^\mu T^A d_t)$
$(\bar{L}R)(\bar{R}L)$ and $(\bar{L}R)(\bar{L}R)$		B -violating			
Q_{ledq}	$(\bar{l}_p^j e_r)(\bar{d}_s q_t^j)$	Q_{duq}	$\varepsilon^{\alpha\beta\gamma} \varepsilon_{jk} [(d_p^\alpha)^T C u_r^\beta] [(q_s^{\gamma j})^T C l_t^k]$		
$Q_{quqd}^{(1)}$	$(\bar{q}_p^j u_r) \varepsilon_{jk} (\bar{q}_s^k d_t)$	Q_{qqu}	$\varepsilon^{\alpha\beta\gamma} \varepsilon_{jk} [(q_p^{\alpha j})^T C q_r^{\beta k}] [(u_s^\gamma)^T C e_t]$		
$Q_{quqd}^{(8)}$	$(\bar{q}_p^j T^A u_r) \varepsilon_{jk} (\bar{q}_s^k T^A d_t)$	$Q_{qqq}^{(1)}$	$\varepsilon^{\alpha\beta\gamma} \varepsilon_{jk} \varepsilon_{mn} [(q_p^{\alpha j})^T C q_r^{\beta k}] [(q_s^{\gamma m})^T C l_t^n]$		
$Q_{lequ}^{(1)}$	$(\bar{l}_p^j e_r) \varepsilon_{jk} (\bar{q}_s^k u_t)$	$Q_{qqq}^{(3)}$	$\varepsilon^{\alpha\beta\gamma} (\tau^I \varepsilon)_{jk} (\tau^I \varepsilon)_{mn} [(q_p^{\alpha j})^T C q_r^{\beta k}] [(q_s^{\gamma m})^T C l_t^n]$		
$Q_{lequ}^{(3)}$	$(\bar{l}_p^j \sigma_{\mu\nu} e_r) \varepsilon_{jk} (\bar{q}_s^k \sigma^{\mu\nu} u_t)$	Q_{duu}	$\varepsilon^{\alpha\beta\gamma} [(d_p^\alpha)^T C u_r^\beta] [(u_s^\gamma)^T C e_t]$		

Table 2: Dimension-six four-fermion operators from Ref. [45]. Generation indices p, r, s, t are explicitly displayed for all fermion fields. The operator names in the left column of each block should be supplemented with generation indices of the fermion fields whenever necessary, e.g., $Q_{lq}^{(1)} \rightarrow Q_{lq}^{(1)prst}$. Dirac indices are always contracted within the brackets, and not displayed. The same is true for the isospin and colour indices in the upper part of the table. In the lower-left block of that table, colour indices are still contracted within the brackets, while the isospin ones are made explicit. Colour indices are displayed only for operators that violate the baryon number B (lower-right block).

To our knowledge, no complete classification of operators of dimension higher than six exists. However, a notable exception concerns operators that violate total lepton number, which start at dimension five as discussed above. The lepton number violating (LNV) operators up to and including dimension eleven have been classified in Ref. [50], that also studied the contribution of these operators to various LNV processes, from low-energy to collider physics. Among the LNV operator, of particular interests are the $\Delta L = 2$ six-fermion operators involving four quark field and two lepton fields that contribute to neutrino-less double beta decay ($dd \rightarrow uuee$ at the quark-lepton level), that have also been studied in Ref. [51], although in a non SU(2) invariant framework. If the scale of LNV is close to the TeV scale, these operators can contribute to neutrino-less double beta decay rate at a level that will be probed in the next-generation experiments. The associated nuclear matrix elements are quite different from those arising in the standard Majorana neutrino exchange and have been studied in Ref. [51].

4 Discovery, Diagnosis, and Interpretability

As discussed in Section 1, the processes of interest to this volume naturally fall into three broad categories: (a) rare and forbidden processes; (b) precision tests; and (c) cosmological and astrophysical

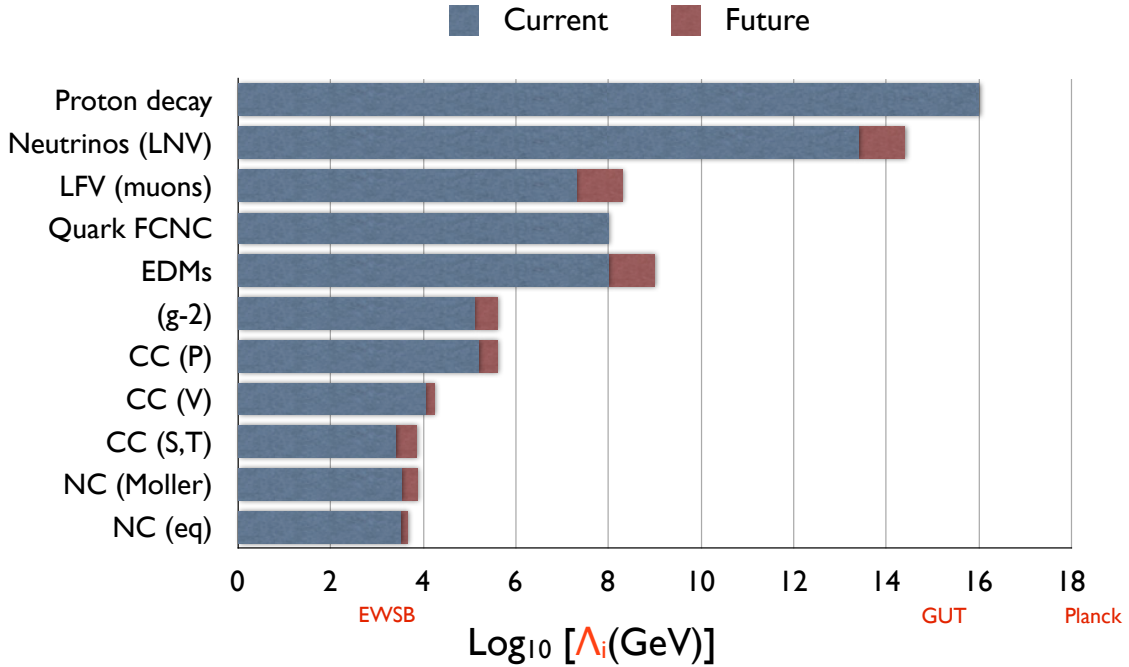


Figure 2: Summary of current and future constraints on the effective new physics scale Λ_i defined in Eq. (3.59) arising from various low-energy observables. Note that the Λ_i absorb the Wilson coefficients and do not necessarily represent the masses of new degrees of freedom that become active at high energy scales.

probes. In the preceding sections of this introductory article, we have attempted to set a framework for the interpretation of results. The baseline is sufficiently reliable knowledge of SM expectations, often at the level of electroweak radiative corrections. The effects of BSM physics can be classified in a model-independent way in terms of effective operators of successively higher mass dimension with coefficients proportional to appropriate inverse powers of Λ . Of course, for BSM dynamics involving new light degrees of freedom as in possible super-light gauge bosons that might account for the a_μ discrepancy, the effective operator analysis is not appropriate. Moreover, when the new degrees of freedom are not much heavier than the weak scale and enter at the loop level, the expansion of Eq. (3.56) may not be optimal. The discussion of the supersymmetric loop contributions to charged current and neutral current observables in the corresponding reviews would constitute an example of the latter situation.

Broadly speaking, the three classes of low-energy studies provide new opportunities for significant discoveries, tools for diagnosing the detailed nature of BSM physics if it is observed, and/or placing strong constraints on various possibilities. The task of diagnosing and constraining BSM physics requires that one have in hand sufficient theoretical control over SM processes so that poorly-known aspects of the latter do not generate confusion about the former. We have already alluded to the QCD-related uncertainties that enter SM electroweak radiative corrections for CC and NC processes. The analogous strong interaction uncertainties that impact the interpretation of the muon anomalous magnetic moment are well-known. Here, we summarize the corresponding theoretical challenges as they bear on the prospects for discovery and diagnosis in the topics discussed in the remainder of this volume.

Electric Dipole Moment Searches. The observation of a non-zero permanent electric dipole moment (EDM) of a polar molecule, neutral atom, nucleon, or nucleus would represent a major discovery. The sensitivity of the next generation of experiments would not reach the level of sensitivity needed to probe the effects of SM CKM CP-violation. Consequently, a non-vanishing EDM would point to the effects of the QCD θ -term and/or BSM CP-violation. As discussed above, the mass scale of BSM interactions probed in the next generation of EDM searches is approaching the tens of TeV level.

The theoretical challenge for the EDM program is not to make room for discovery. It is, rather, to provide a path to diagnosing the underlying mechanism should a non-vanishing EDM be observed, or to set the framework for constraining possible sources of BSM CP-violation in the event of non-observation of EDMs in the next generation of experiments. At the level of the effective operators introduced here, one encounters twelve possible sources of BSM CP-violation involving the first generation quarks and leptons, photons, and gluons. These possible sources are summarized in Table I of the EDM review [52]. Polar molecules and paramagnetic atoms are in general sensitive to four different operators, though in practice are dominated by only two of the four: the electron EDM and a combination of the semileptonic four fermion operators: Q_{ledq} and $Q_{lequ}^{(1)}$. Diamagnetic atoms, nucleons, and nuclei probe the θ -term, quark EDMs, and six other dimension-six CPV operators. One component of the theoretical challenge is to identify a sufficient number of systems with complementary dependences on these operators to allow one to disentangle them should an EDM be observed in any one system. As discussed in the EDM review, a promising new direction in this regard are light nuclei whose EDMs may be probed in storage ring experiments.

The other theoretical challenge involves matching the underlying CPV operators onto hadronic, nuclear, and atomic degrees of freedom. While the theoretical uncertainties associated with many-body atomic computations appears to be reasonably small, the same cannot be said regarding the hadronic and nuclear uncertainties. In diamagnetic atoms such as ^{199}Hg , the atomic EDM is most sensitive to the nuclear Schiff moment. The latter, in turn, arises from long-range time-reversal (TV) and parity-violating (PV) pion-exchange interactions that are induced by the non-leptonic CPV operators. Carrying out robust nuclear many-body computations of the Schiff moment remains a key theoretical challenge. The matching of the dimension six operators onto TVPV πNN interactions and the nucleon EDMs constitutes a similar direction need of concerted theoretical effort. In some cases, the uncertainty associated with this matching is an order of magnitude or larger, as discussed in the EDM review [52]. We direct the reader to Table 6 of that article, where a summary of “best values” and “reasonable ranges” for the relevant hadronic matrix elements may be found.

Probes of Lepton Number and Flavor Violation. The physics responsible for neutrino masses and lepton mixing remains unknown, and it can be uniquely probed by searches for lepton flavor violation (LFV) in charged-lepton processes ($\mu \rightarrow e\gamma$, $\mu \rightarrow e\bar{e}e$, $\mu \rightarrow e$ conversion in nuclei, $\tau \rightarrow (e, \mu)\gamma$, $\tau \rightarrow (e, \mu)+$ hadrons, etc.), and lepton number violation (LNV) in neutrino-less double beta decays. Given the tiny (for charged LFV) or null (for LNV) SM background, these are “discovery” searches, albeit experimentally extremely challenging. Both positive or null results from these searches will provide unique information about the symmetry structure of physics beyond the SM, whether or not the LHC detects new degrees of freedom at the TeV scale.

Charged LFV processes involving muons and tau are theoretically very clean: the atomic, nuclear, (for $\mu \rightarrow e$ conversion), and hadronic (for $\tau \rightarrow (e, \mu)+$ hadrons) effects are under reasonable control. Therefore, charged LFV processes are not only discovery channels, but also powerful diagnostic tools. As an example, the physics reach of $\mu \rightarrow e\gamma$, $\mu \rightarrow e\bar{e}e$, and $\mu \rightarrow e$ conversion in nuclei, and their complementarity are illustrated in Figures 2 and 3 of the review on lepton number

and flavor violation [53]. If observed, the relative rates of various $\mu \rightarrow e$ or $\tau \rightarrow (e, \mu)$ processes will provide information about the underlying mechanism (e.g. whether the dipole operator or other structures dominate). Similarly, comparing $\mu \rightarrow e$ with $\tau \rightarrow (e, \mu)$ transitions will point to the structure of the underlying sources of flavor breaking.

LNV is most sensitively probed by neutrino-less double beta decay. Observation of such process would indicate that lepton number is not conserved and that neutrinos are their own antiparticles. Here the (inter-related) theoretical challenges are: (i) diagnosing the underlying mechanism (light Majorana neutrino mediator, or new low-scale source of LNV); (ii) within a given mechanism, reducing the uncertainty in the nuclear matrix elements, which is key to extracting bounds on the underlying model parameters (for example $\langle m_{\beta\beta} \rangle$ if the mechanism is the exchange of a light Majorana neutrino). Both these issues are discussed at depth in Ref. [53], and the status of nuclear matrix elements is summarized in their Figure 8.

Charged and Neutral Current Processes. The emphasis of precise studies of weak decays and neutral current processes lies on diagnosing key aspects of possible BSM physics, should a discovery be made at the energy frontier. Conversely, agreement of these studies with SM expectations can place severe constraints on BSM scenarios. Within the Minimal Supersymmetric Standard Model, for example, a comparison of weak charges of the proton and electron as measured in PV electron scattering could yield information as to whether the MSSM violates or respects $B - L$ (see Figure 10 of the NC review [25]). Alternately, a comparison of the results of first row CKM unitarity tests with those of pion leptonic decays could yield information on the spectrum of supersymmetric particles (see Figure 6 of the weak decay review). Studies of the PV asymmetries could also yield insights into the nature of new neutral gauge bosons (Z'), such as in string-theory motivated scenarios. In each case, the low-energy studies have the potential to complement what one may learn from collider studies. Deep inelastic PV electron-deuteron scattering has a unique sensitivity to a light, “leptophobic” Z' that is a candidate for explaining recent results from the Tevatron. Conversely, if new particles are too heavy to be produced directly at the LHC or other colliders, the effective operator description would apply equally to the interpretation of collider results and low-energy tests. In this case, one can see directly the power of low-energy measurements to complement the reach at the energy frontier, as illustrated in Figures 3 and 4 of the weak decay review [19].

Discerning the effects of these BSM scenarios will require not only pushing the level of experimental sensitivity to the next decade, but also making similar improvements in the reliability of the theoretical SM inputs. Among the primary challenges are the $W\gamma$ and $Z\gamma$ box graphs that enter the extraction of V_{ud} from neutron and nuclear β -decay and the proton weak charge from elastic PV electron-proton scattering. The interpretation of neutron and nuclear β -decay correlations in terms of non- $(V - A) \otimes (V - A)$ interactions similarly calls for refined computations of the nucleon scalar and tensor form factors (see Figure 3 of the weak decay review [19]). Determining the magnitude of higher-twist corrections and contributions associated with charge symmetry-violation in parton distribution functions would enhance the BSM diagnostic power of PV deep inelastic electron scattering.

Neutrinos: Terrestrial, Astrophysical, and Cosmological Probes. Neutrinos probe a rich sector of the BSM dynamics, largely inaccessible at the high-energy frontier. In the EFT language used in this review, neutrino experiments probe both the particle content and symmetry structure of the EFT, through question such as: are there light sterile right-handed neutrinos? How many? If so, do they acquire a Majorana mass term (dimension-three lepton-number violating operator), and do they have Yukawa interactions with Higgs and left-handed leptons (dimension-four operator)? Is there a direct Majorana mass term for left-handed neutrinos (dimension-five operator of

Eq. (3.58))? Is CP symmetry violated by the above couplings?

Regardless the origin of the light neutrino mass matrix (Dirac or Majorana), as discussed in Ref. [54], through oscillation experiments involving solar, atmospheric, reactor, and accelerator neutrinos we know a great deal about the mixing angles and mass-splitting of the three active neutrinos. In terms of determining neutrino properties, besides the Majorana or Dirac nature, the remaining open questions concern the overall mass scale, the mass hierarchy, and CP violation in the mixing matrix, and the possibility of sterile states or non-standard neutrino-matter interactions. It is also worth pointing out that now it has become possible to use neutrinos as quantitative astrophysical probes of the Sun and the Standard Solar Model, as discussed in the neutrino oscillation review [54].

Last but not least, as discussed in the review on neutrinos in cosmology and astrophysics [55], neutrinos shape key aspects of the Early Universe and core collapse supernovae dynamics, because they carry a dominant fraction of the total energy and entropy in these environments. Given the energy and flavor-dependence of neutrino processes in the EU or SN, the key open theoretical challenge involves understanding neutrino flavor transformation in medium (including coherent and incoherent scattering). A robust understanding of this problem will allow us to (i) combine recent and future developments in observational cosmology and neutrino experiment to probe the presence of new physics in the neutrino sector (e.g. sterile neutrinos); (ii) reliably predict the flavor and spectral composition of SN neutrino signal; (iii) explore the origin of the lightest and heaviest nuclei, through nucleosynthesis in the early universe and astrophysical sites.

Dark Matter and Nuclear Physics. Dark matter (DM) provides approximately one-fifth of the mass-energy content of the Universe and the SM has no candidate for it. Several theoretically well-motivated SM extensions contain DM candidates. However, the constraints of relic density, stability (on cosmological time scales), and extremely weak coupling to ordinary matter still leave many open possibilities. While “WIMPs” (weakly interacting massive particles) remain a very attractive candidate for DM, as illustrated in Figure 1 of the review article [56], the mass and interaction strengths of DM candidates span fifty orders of magnitude! Reference [56] discusses how nuclear physics can play an important role in both WIMP and non-WIMP DM searches. For WIMP direct detection searches, one obvious challenge for nuclear theory is the calculation of WIMP-nucleus cross sections starting from quark-WIMP interactions. Similarly, facilities dedicated to nuclear physics are well-poised to investigate certain non-WIMP models, such as “Hidden Sector Models”. In parallel to this, developments in observational cosmology permit probes of the relativistic energy density at early epochs and thus provide new ways to constrain dark-matter models, provided nuclear physics inputs are sufficiently well-known. The emerging confluence of accelerator, astrophysical, and cosmological constraints permit searches for dark-matter candidates in a greater range of masses and interaction strengths than heretofore possible.

Hadronic Parity-Violation. Apart from these BSM probes, low-energy electroweak interactions continue to provide unique windows on poorly understood aspects of nucleon and nuclear structure. In this series of reviews we have not emphasized this aspect of the low-energy program, but have included one article in this spirit focusing on hadronic PV [57]. The nonleptonic weak interaction in the SM remains a topic of considerable interest as it challenges our understanding of the interplay of strong and weak interactions. More broadly, several puzzles remain to be addressed, such as the origin of the $\Delta I = 1/2$ rule in non-leptonic weak decays of mesons; the tension between S - and P -wave amplitudes in strangeness changing, non-leptonic hyperon decays; and the enhanced PV asymmetries in strangeness-changing radiative hyperon decays. Whether the origin of these puzzles lies in the role played by the strange quark in hadronic dynamics of something not yet

identified at the interface of quark-quark weak interactions and non-perturbative QCD remains an open question.

The study of the strangeness conserving hadronic weak interaction (HWI) provides a probe of these underlying dynamics without the presence of the strange quark. Theoretically, one may characterize the HWI in terms of a low-energy effective field theory involving nucleon and – for appropriate energy scales – pion degrees of freedom. An alternate, model-dependent approach based on meson-exchange interactions has been widely used to interpret the experimental results (a detailed translation between the two approaches appears in Ref. [57]). Either way, the goal of the combined experimental and theoretical program is to obtain from measurements values for the hadronic-level parameters that may then be matched onto the underlying non-leptonic, strangeness conserving HWI. The review of hadronic PV outlines progress and opportunities in this program [57]. In particular, results of an updated global analysis in terms of the meson-exchange model parameters appears in Figure 3 of Ref. [57]. The matching of the effective hadronic parameters onto the quark-level HWI remains an open theoretical challenge.

5 Conclusion

We now leave it to the reader to delve into the details of each of the aforementioned directions. Suffice it to say, the program of low-energy probes of BSM physics and related topics is a rich, diverse, and multidisciplinary field of research. These studies provide a powerful and unique window on dynamics at high energy scales and have the potential to uncover key aspects of new laws of nature that may have been more apparent in the early universe than they are today. Their physics reach complements that of experiments at the energy and cosmic frontiers. They present a number of theoretically compelling challenges. We hope that this series of articles will give the reader a taste of the opportunities and excitement that the field engenders.

References

- [1] Jens Erler and Michael J. Ramsey-Musolf. Low energy tests of the weak interaction. *Prog.Part.Nucl.Phys.*, 54:351–442, 2005, doi:10.1016/j.ppnp.2004.08.001, arXiv:hep-ph/0404291.
- [2] M.J. Ramsey-Musolf and S. Su. Low Energy Precision Test of Supersymmetry. *Phys.Rept.*, 456:1–88, 2008, doi:10.1016/j.physrep.2007.10.001, arXiv:hep-ph/0612057.
- [3] Maxim Pospelov and Adam Ritz. Electric dipole moments as probes of new physics. *Annals Phys.*, 318:119–169, 2005, doi:10.1016/j.aop.2005.04.002, arXiv:hep-ph/0504231.
- [4] Steven R. Elliott and Petr Vogel. Double beta decay. *Ann.Rev.Nucl.Part.Sci.*, 52:115–151, 2002, doi:10.1146/annurev.nucl.52.050102.090641, arXiv:hep-ph/0202264.
- [5] Steven R. Elliott and Jonathan Engel. Double beta decay. *J.Phys.*, G30:R183, 2004, doi:10.1088/0954-3899/30/9/R01, arXiv:hep-ph/0405078.
- [6] III Avignone, Frank T., Steven R. Elliott, and Jonathan Engel. Double Beta Decay, Majorana Neutrinos, and Neutrino Mass. *Rev.Mod.Phys.*, 80:481–516, 2008, doi:10.1103/RevModPhys.80.481, arXiv:0708.1033.
- [7] P. Herczeg. Beta decay beyond the standard model. *Prog.Part.Nucl.Phys.*, 46:413–457, 2001, doi:10.1016/S0146-6410(01)00149-1.

- [8] Nathal Severijns, Marcus Beck, and Oscar Naviliat-Cuncic. Tests of the standard electroweak model in beta decay. *Rev.Mod.Phys.*, 78:991–1040, 2006, doi:10.1103/RevModPhys.78.991, arXiv:nucl-ex/0605029.
- [9] Nathal Severijns and Oscar Naviliat-Cuncic. Symmetry tests in nuclear beta decay. *Ann.Rev.Nucl.Part.Sci.*, 61:23–46, 2011, doi:10.1146/annurev-nucl-102010-130410.
- [10] K.S. Kumar, Sonny Mantry, W.J. Marciano, and P.A. Souder. Low Energy Measurements of the Weak Mixing Angle. 2013, arXiv:1302.6263.
- [11] M.J. Musolf, T.W. Donnelly, J. Dubach, S.J. Pollock, S. Kowalski, et al. Intermediate-energy semileptonic probes of the hadronic neutral current. *Phys.Rept.*, 239:1–178, 1994, doi:10.1016/0370-1573(94)90040-X.
- [12] E.G. Adelberger and W.C. Haxton. Parity Violation in the Nucleon-Nucleon Interaction. *Ann.Rev.Nucl.Part.Sci.*, 35:501–558, 1985.
- [13] Michael J. Ramsey-Musolf and Shelley A. Page. Hadronic parity violation: A New view through the looking glass. *Ann.Rev.Nucl.Part.Sci.*, 56:1–52, 2006, doi:10.1146/annurev.nucl.54.070103.181255, arXiv:hep-ph/0601127.
- [14] A. Sirlin. Current Algebra Formulation of Radiative Corrections in Gauge Theories and the Universality of the Weak Interactions. *Rev.Mod.Phys.*, 50:573, 1978, doi:10.1103/RevModPhys.50.573.
- [15] W.J. Marciano and A. Sirlin. Radiative Corrections to beta Decay and the Possibility of a Fourth Generation. *Phys.Rev.Lett.*, 56:22, 1986, doi:10.1103/PhysRevLett.56.22.
- [16] William J. Marciano and A. Sirlin. Radiative corrections to pi(lepton 2) decays. *Phys.Rev.Lett.*, 71:3629–3632, 1993, doi:10.1103/PhysRevLett.71.3629.
- [17] William J. Marciano and Alberto Sirlin. Improved calculation of electroweak radiative corrections and the value of V_{ud} . *Phys.Rev.Lett.*, 96:032002, 2006, doi:10.1103/PhysRevLett.96.032002, arXiv:hep-ph/0510099.
- [18] A.N. Ivanov, M. Pitschmann, and N.I. Troitskaya. Neutron Beta-Decay as Laboratory for Test of Standard Model. 2012, arXiv:1212.0332.
- [19] Vincenzo Cirigliano, Susan V. Gardner, and Barry R. Holstein. Beta Decays and Non-Standard Interactions in the LHC Era. 2013, arXiv:1303.6953.
- [20] W.J. Marciano and A. Sirlin. Radiative Corrections to Neutrino Induced Neutral Current Phenomena in the SU(2)-L x U(1) Theory. *Phys.Rev.*, D22:2695, 1980, doi:10.1103/PhysRevD.31.213, 10.1103/PhysRevD.22.2695.
- [21] W.J. Marciano and A. Sirlin. RADIATIVE CORRECTIONS TO ATOMIC PARITY VIOLATION. *Phys.Rev.*, D27:552, 1983, doi:10.1103/PhysRevD.27.552.
- [22] S. Sarantakos, A. Sirlin, and W.J. Marciano. Radiative Corrections to Neutrino-Lepton Scattering in the SU(2)-L x U(1) Theory. *Nucl.Phys.*, B217:84, 1983, doi:10.1016/0550-3213(83)90079-2.
- [23] W.J. Marciano and A. Sirlin. On Some General Properties of the O(alpha) Corrections to Parity Violation in Atoms. *Phys.Rev.*, D29:75, 1984, doi:10.1103/PhysRevD.29.75, 10.1103/PhysRevD.31.213.2.

- [24] M.J.G. Veltman. Limit on Mass Differences in the Weinberg Model. *Nucl.Phys.*, B123:89, 1977, doi:10.1016/0550-3213(77)90342-X.
- [25] Jens Erler and Shufang Su. The Weak Neutral Current. 2013, arXiv:1303.5522.
- [26] Andrzej Czarnecki and William J. Marciano. Electroweak radiative corrections to polarized Moller scattering asymmetries. *Phys.Rev.*, D53:1066–1072, 1996, doi:10.1103/PhysRevD.53.1066, arXiv:hep-ph/9507420.
- [27] Jens Erler and Michael J. Ramsey-Musolf. The Weak mixing angle at low energies. *Phys.Rev.*, D72:073003, 2005, doi:10.1103/PhysRevD.72.073003, arXiv:hep-ph/0409169.
- [28] Ya.B. Zeldovich. *Sov.Phys. JETP*, 6:1184, 1958.
- [29] M.J. Musolf and Barry R. Holstein. Observability of the anapole moment and neutrino charge radius. *Phys.Rev.*, D43:2956–2970, 1991, doi:10.1103/PhysRevD.43.2956.
- [30] A. Kurylov, M.J. Ramsey-Musolf, and S. Su. Probing supersymmetry with parity violating electron scattering. *Phys.Rev.*, D68:035008, 2003, doi:10.1103/PhysRevD.68.035008, arXiv:hep-ph/0303026.
- [31] Michael E. Peskin and Tatsu Takeuchi. A New constraint on a strongly interacting Higgs sector. *Phys.Rev.Lett.*, 65:964–967, 1990, doi:10.1103/PhysRevLett.65.964.
- [32] Mitchell Golden and Lisa Randall. RADIATIVE CORRECTIONS TO ELECTROWEAK PARAMETERS IN TECHNICOLOR THEORIES. *Nucl.Phys.*, B361:3–23, 1991, doi:10.1016/0550-3213(91)90614-4.
- [33] William J. Marciano and Jonathan L. Rosner. Atomic parity violation as a probe of new physics. *Phys.Rev.Lett.*, 65:2963–2966, 1990, doi:10.1103/PhysRevLett.65.2963.
- [34] D.C. Kennedy and Paul Langacker. Precision electroweak experiments and heavy physics: A Global analysis. *Phys.Rev.Lett.*, 65:2967–2970, 1990, doi:10.1103/PhysRevLett.65.2967.
- [35] D.C. Kennedy and Paul Langacker. Precision electroweak experiments and heavy physics: An Update. *Phys.Rev.*, D44:1591–1592, 1991, doi:10.1103/PhysRevD.44.1591.
- [36] Guido Altarelli and Riccardo Barbieri. Vacuum polarization effects of new physics on electroweak processes. *Phys.Lett.*, B253:161–167, 1991, doi:10.1016/0370-2693(91)91378-9.
- [37] B. Holdom and J. Terning. Large corrections to electroweak parameters in technicolor theories. *Phys.Lett.*, B247:88–92, 1990, doi:10.1016/0370-2693(90)91054-F.
- [38] Kaoru Hagiwara, S. Matsumoto, D. Haidt, and C.S. Kim. A Novel approach to confront electroweak data and theory. *Z.Phys.*, C64:559–620, 1994, doi:10.1007/BF01957770, arXiv:hep-ph/9409380.
- [39] Jens Erler, Andriy Kurylov, and Michael J Ramsey-Musolf. The Weak charge of the proton and new physics. *Phys.Rev.*, D68:016006, 2003, doi:10.1103/PhysRevD.68.016006, arXiv:hep-ph/0302149.
- [40] Thomas Appelquist and Guo-Hong Wu. The Electroweak chiral Lagrangian and new precision measurements. *Phys.Rev.*, D48:3235–3241, 1993, doi:10.1103/PhysRevD.48.3235, arXiv:hep-ph/9304240.
- [41] Anthony C. Longhitano. Heavy Higgs Bosons in the Weinberg-Salam Model. *Phys.Rev.*, D22:1166, 1980, doi:10.1103/PhysRevD.22.1166.

- [42] F. Feruglio. The Chiral approach to the electroweak interactions. *Int.J.Mod.Phys.*, A8:4937–4972, 1993, doi:10.1142/S0217751X93001946, arXiv:hep-ph/9301281.
- [43] Jose Wudka. Electroweak effective Lagrangians. *Int.J.Mod.Phys.*, A9:2301–2362, 1994, doi:10.1142/S0217751X94000959, arXiv:hep-ph/9406205.
- [44] Steven Weinberg. Baryon and Lepton Nonconserving Processes. *Phys.Rev.Lett.*, 43:1566–1570, 1979, doi:10.1103/PhysRevLett.43.1566.
- [45] B. Grzadkowski, M. Iskrzynski, M. Misiak, and J. Rosiek. Dimension-Six Terms in the Standard Model Lagrangian. *JHEP*, 1010:085, 2010, doi:10.1007/JHEP10(2010)085, arXiv:1008.4884.
- [46] Frank Wilczek and A. Zee. Operator Analysis of Nucleon Decay. *Phys.Rev.Lett.*, 43:1571–1573, 1979, doi:10.1103/PhysRevLett.43.1571.
- [47] W. Buchmuller and D. Wyler. Effective Lagrangian Analysis of New Interactions and Flavor Conservation. *Nucl. Phys.*, B268:621, 1986, doi:10.1016/0550-3213(86)90262-2.
- [48] Nicole F. Bell, Mikhail Gorchtein, Michael J. Ramsey-Musolf, Petr Vogel, and Peng Wang. Model independent bounds on magnetic moments of Majorana neutrinos. *Phys.Lett.*, B642:377–383, 2006, doi:10.1016/j.physletb.2006.09.055, arXiv:hep-ph/0606248.
- [49] Zurab Berezhiani and Anna Rossi. Limits on the nonstandard interactions of neutrinos from $e^+ e^-$ colliders. *Phys.Lett.*, B535:207–218, 2002, doi:10.1016/S0370-2693(02)01767-7, arXiv:hep-ph/0111137.
- [50] Andre de Gouvea and James Jenkins. A Survey of Lepton Number Violation Via Effective Operators. *Phys.Rev.*, D77:013008, 2008, doi:10.1103/PhysRevD.77.013008, arXiv:0708.1344.
- [51] Gary Prezeau, M. Ramsey-Musolf, and Petr Vogel. Neutrinoless double beta decay and effective field theory. *Phys.Rev.*, D68:034016, 2003, doi:10.1103/PhysRevD.68.034016, arXiv:hep-ph/0303205.
- [52] Jonathan Engel, Michael J. Ramsey-Musolf, and U. van Kolck. Electric Dipole Moments of Nucleons, Nuclei, and Atoms: The Standard Model and Beyond. 2013, arXiv:1303.2371.
- [53] Andre de Gouvea and Petr Vogel. Lepton Flavor and Number Conservation, and Physics Beyond the Standard Model. 2013, arXiv:1303.4097.
- [54] A.B. Balantekin and W.C. Haxton. Neutrino Oscillations. 2013, arXiv:1303.2272.
- [55] A.B. Balantekin and G.M. Fuller. Neutrinos in Cosmology and Astrophysics. 2013, arXiv:1303.3874.
- [56] Susan Gardner and George Fuller. Dark Matter Studies Entrain Nuclear Physics. 2013, arXiv:1303.4758.
- [57] W.C. Haxton and B.R. Holstein. Hadronic Parity Violation. 2013, arXiv:1303.4132.